SANDIA NATIONAL LABORATORIES
WASTE ISOLATION PILOT PLANT

ANALYSIS REPORT FOR DIRECT BRINE RELEASES IN THE 2026 COMPLIANCE RECERTIFICATION APPLICATION PERFORMANCE ASSESSMENT: INTERIM STATE REPOSITORY

REVISION 0

TODD ZEITLER
(Affiliate)

Digitally signed by TODD ZEITLER
(Affiliate)
Date: 2025.09.16 08:34:49 -06'00'

Authentication

Author:	Todd R. Zeitler	Org.	08912
Technical Reviewer:	Brad Day	Org.	08881
QA Reviewer:	Shelly Nielsen	Org.	08883
Management Reviewer:	Steve Wagner	Org.	08881

SEPTEMBER 2025

Information Only

Executive Summary

The Waste Isolation Pilot Plant (WIPP) was initially certified as a repository consisting of 10 panels, which were excavated for the long-term storage and placement of transuranic waste (U.S. EPA 1998). However, due to operational constraints, the entire volume of the 10 panels is no longer available for waste disposal. In March 2024, the U.S. Department of Energy (DOE) submitted the Replacement Panels Planned Change Request (RPPCR) to the U.S. Environmental Protection Agency (EPA) for approval of waste emplacement in two new panels. These panels, referred to as replacement panels, are located to the west of the existing operations area. The EPA approved the RPPCR in July 2025.

The addition of the two replacement panels is not expected to provide adequate space for the disposal of the allowable waste volume designated for WIPP under the Land Withdrawal Act (LWA); thus, the 12-panel configuration is regarded as an interim state of the repository. The DOE may pursue approval for waste disposal in seven additional panels to accommodate the full allowable volume of waste. This hypothetical 19-panel configuration is considered the anticipated final state of the repository.

The DOE demonstrates compliance with containment requirements as outlined in the Certification Criteria of Title 40 CFR Part 191.13 through performance assessment (PA). PA calculations estimate the probability and consequences of potential radionuclide releases from the repository to the accessible environment over a regulatory period of 10,000 years following facility closure. WIPP PA models are utilized to support the periodic recertification of WIPP.

The 2026 Compliance Recertification Application (CRA-2026) represents the fifth recertification application submitted to the EPA. A PA has been carried out by Sandia National Laboratories to support the DOE's submission of the CRA-2026. The results presented in the CRA-2026 PA are compared to those from the RPPCR PA, the most recent regulatory submission.

This analysis report documents the direct brine release (DBR) volume component of the CRA-2026 PA for the interim state repository. This report details the effects of the changes introduced and incorporated in the CRA-2026 PA that impact the DBR model. In comparison to the RPPCR PA, the primary effects of these changes are a decreased number of non-zero DBR volumes across all scenarios, decreased overall mean non-zero release volume (including for intrusions with a Castile intersection), and increased maximum release volumes for all scenarios with a previous intrusion.

Information Only

TABLE OF CONTENTS

EXECUTIVE SUMMARY II

1.0 INTRODUCTION 7

2.0 CHANGES SINCE THE RPPCR 8

2.1 Repository Design 8
2.2 Parameters Related to Repository Dimensions 10
2.3 Updates to the Salado Flow and Transport Computational Grid 10
2.4 Waste Inventory 11
2.5 Baseline Actinide Solubilities 11
2.6 Solubility Uncertainty Distributions 12
2.7 Colloidal Enhancement Parameters 12
2.8 MgO Hydration Parameters 12
2.9 Lower Bound on Capillary Pressure in the Anhydrite Marker Beds 12
2.10 Porosity-Permeability Parameter Distribution 13
2.11 Parameters Not Updated as Anticipated in Analysis Plan AP-214 13

3.0 CONCEPTUAL APPROACH FOR THE CRA-2026 14

3.1 Model Geometry 16
3.2 Initial Conditions 17

4.0 DBR METHODOLOGY 19

4.1 Modeled Scenarios 19
4.2 Code Execution and Run Control 20

5.0 RESULTS 21

5.1 Summary 21
5.2 S1-DBR 27
5.3 S2-DBR 30
5.4 S4-DBR 33
5.5 Maximum Releases 36

6.0 DRIVERS AND CORRELATIONS 38

6.1 Initial Conditions Summary 38

Information Only

6.1.1 S2-DBR 38
6.1.2 S4-DBR 43
6.2 Correlation and Sensitivity to Initial Conditions 47

7.0 SUMMARY 52

8.0 REFERENCES 54

9.0 APPENDIX A – SENSITIVITY TO INPUT PARAMETERS 57

10.0 APPENDIX B – ADDITIONAL REPLICATE 1 TABLES AND PLOTS 60

10.1 S3-DBR 60
10.2 S5-DBR 62

11.0 APPENDIX C –REPLICATE COMPARISON 64

LIST OF FIGURES

Figure 1. Interim State Repository Layout 9
Figure 2. CRA26_IS Salado Flow and Transport Computational Grid 11
Figure 3. CRA26_IS and RPPCR DBR Grid with Simulated Intrusion Locations 17
Figure 4. Regions Used to Transfer Initial Pressure and Saturation from the BRAGFLO Salado Grid to the DBR Grid 18
Figure 5. DBR Run Control Diagram 20
Figure 6. Release Volume Frequency, All Non-Zero Releases, Replicate 1 25
Figure 7. Release Volumes, All Non-Zero Releases, Replicate 1 25
Figure 8. Release Volumes by Scenario, All Non-Zero Releases, Replicate 1 26
Figure 9. Number of Non-Zero DBR Events by Scenario, Replicate 1 26
Figure 10. S1-DBR Volumes, All Non-Zero Releases, Replicate 1 29
Figure 11. S2-DBR Volumes, All Non-Zero Releases, Replicate 1 32
Figure 12. S4-DBR Volumes, All Non-Zero Releases, Replicate 1 35
Figure 13. S2-DBR Brine Pressure, All Intrusions, Replicate 1 41
Figure 14. S2-DBR Brine Saturation, All Intrusions, Replicate 1 42
Figure 15. S4-DBR Brine Pressure, All Intrusions, Replicate 1 45
Figure 16. S4-DBR Brine Saturation, All Intrusions, Replicate 1 46

Information Only

Figure 17. S2-DBR Release Volume Versus Brine Pressure, All Non-Zero Intrusions, Replicate 1 49
Figure 18. S2-DBR Release Volume Versus Brine Saturation, All Non-Zero Intrusions, Replicate 1.....50
Figure 19. Brine Saturation Frequency, S2-DBR All Lower and Middle Intrusions, Replicate 1 51
Figure 20. Brine Saturation Frequency, S2-DBR All Upper and Other Intrusions, Replicate 1 ...51
Figure 21. Halite Porosity Versus Brine Release Volume for Location “L”, Scenario S2-DBR, Time 10,000 Years, Replicate 1.....58
Figure 22. Borehole Permeability Versus Brine Release Volume for Location “L”, Scenario S2-DBR, Time 10,000 Years, Replicate 1 58
Figure 23. DRZ Permeability Versus Brine Release Volume for Location “L”, Scenario S2-DBR, Time 10,000 Years, Replicate 1.....59
Figure 24. Castile Brine Pressure Versus Brine Release Volume for Location “L”, Scenario S2-DBR, Time 550 Years, Replicate 1 59
Figure 25. S3-DBR Volumes, All Non-Zero Releases, Replicate 1.....61
Figure 26. S5-DBR Volumes, All Non-Zero Releases, Replicate 1.....63
Figure 27. Release Volume Frequency, All Non-Zero Releases, Replicate 2.....65
Figure 28. Release Volumes, All Non-Zero Releases, Replicate 2 66
Figure 29. Release Volumes by Scenario, All Non-Zero Releases, Replicate 2 66
Figure 30. Number of Non-Zero DBR Events by Scenario, Replicate 2.....67
Figure 31. Release Volume Frequency, All Non-Zero Releases, Replicate 3.....69
Figure 32. Release Volumes, All Non-Zero Releases, Replicate 3 69
Figure 33. Release Volumes by Scenario, All Non-Zero Releases, Replicate 3 70
Figure 34. Number of Non-Zero DBR Events by Scenario, Replicate 3.....70
Figure 35. Release Volume Frequency, All Non-Zero Releases, All Replicates 71
Figure 36. Release Volumes, All Non-Zero Releases, All Replicates.....71

Information Only

LIST OF TABLES

Table 1. Changed Repository Parameters 10
Table 2. Summary of PA Parameters Used to Compute DBR Volumes 15
Table 3. DBR Scenarios 19
Table 4. DBR Volume Summary, Replicate 1 24
Table 5. S1-DBR Volume Summary, Replicate 1 28
Table 6. S2-DBR Volume Summary, Replicate 1 31
Table 7. S4-DBR volume summary, Replicate 1 34
Table 8. Largest DBR Volumes by Analysis 37
Table 9. S2-DBR Mean Initial Conditions, Replicate 1 40
Table 10. S4-DBR Mean Initial Conditions, Replicate 1 44
Table 11. S3-DBR Volume Summary, Replicate 1 60
Table 12. S5-DBR volume summary, Replicate 1 62
Table 13. DBR Volume Summary, Replicate 2 64
Table 14. DBR Volume Summary, Replicate 3 68

Information Only

1.0 INTRODUCTION

The Waste Isolation Pilot Plant (WIPP), located in southeastern New Mexico, has been developed by the U.S. Department of Energy (DOE) for the geologic disposal of transuranic (TRU) waste. The containment of TRU waste at WIPP is regulated by the U.S. Environmental Protection Agency (EPA) under Title 40 of the Code of Federal Regulations (CFR), Part 191.

The DOE demonstrates compliance with the containment requirements of 40 CFR 191.13 by means of performance assessment (PA) as described in the Certification Criteria of Title 40 CFR Part 194. Sandia National Laboratories (SNL) conducts PAs at the request of the DOE. The PA calculations estimate the probability and consequences of potential radionuclide releases from the repository to the accessible environment over a regulatory period of 10,000 years following facility closure. The PA models are continuously maintained and updated with new information, which typically leads to refinements and modifications in both the models and their parameters. Additionally, planned changes to the repository and its components necessitate updates to the WIPP PA models.

All previous WIPP certifications have been based on a repository consisting of 10 panels. In March 2024, the DOE submitted the Replacement Panels Planned Change Request (RPPCR) to seek EPA approval for waste emplacement in two new panels, referred to as replacement panels, located to the west of the existing operations area (Bollinger 2024). The EPA approved the RPPCR in July 2025 (U.S. EPA 2025).

The addition of the two replacement panels is not expected to provide sufficient space for the disposal of the allowable waste volume designated for WIPP under the Land Withdrawal Act (LWA). The 12-panel configuration is thus regarded as an interim state of the repository. The DOE may seek approval for waste disposal in up to seven additional panels to accommodate the full allowable volume of waste. This 19-panel configuration is considered the anticipated final state of the repository.

The CRA-2026 is the fifth recertification application for the WIPP submitted by the DOE for EPA approval. The PA executed by SNL in support of the CRA-2026 PA is described in AP-214 (Hansen et al. 2025). This analysis report documents the direct brine release (DBR) component of the CRA-2026 PA for the interim state repository.

Information Only

2.0 CHANGES SINCE THE RPPCR

Several changes are incorporated in the CRA-2026 PA relative to the RPPCR that may impact the DBR results, in each case by impacting the brine pressures and brine saturations from the Salado flow calculation (Day 2025) that are used as initial conditions for DBR calculations. These changes include:

- The repository design.
- Parameters related to repository dimensions.
- The waste inventory.
- Baseline actinide solubilities.
- Solubility uncertainty distributions.
- Colloid concentration parameters for humic and microbial colloids.
- MgO hydration parameters.
- The Salado flow and transport computational grid.
- A new lower bound on capillary pressure in the anhydrite marker beds.
- Revisions to the porosity-permeability parameter distribution.

Changes listed above are discussed in more detail in the sections that follow.

2.1 Repository Design

This analysis represents the 12-panel interim state repository consisting of ten original and two replacement panels. Figure 1 depicts the interim state repository. The RPPCR considered the anticipated final repository state, which included a total of 19 waste panels and the entire allowable inventory volume.

Information Only

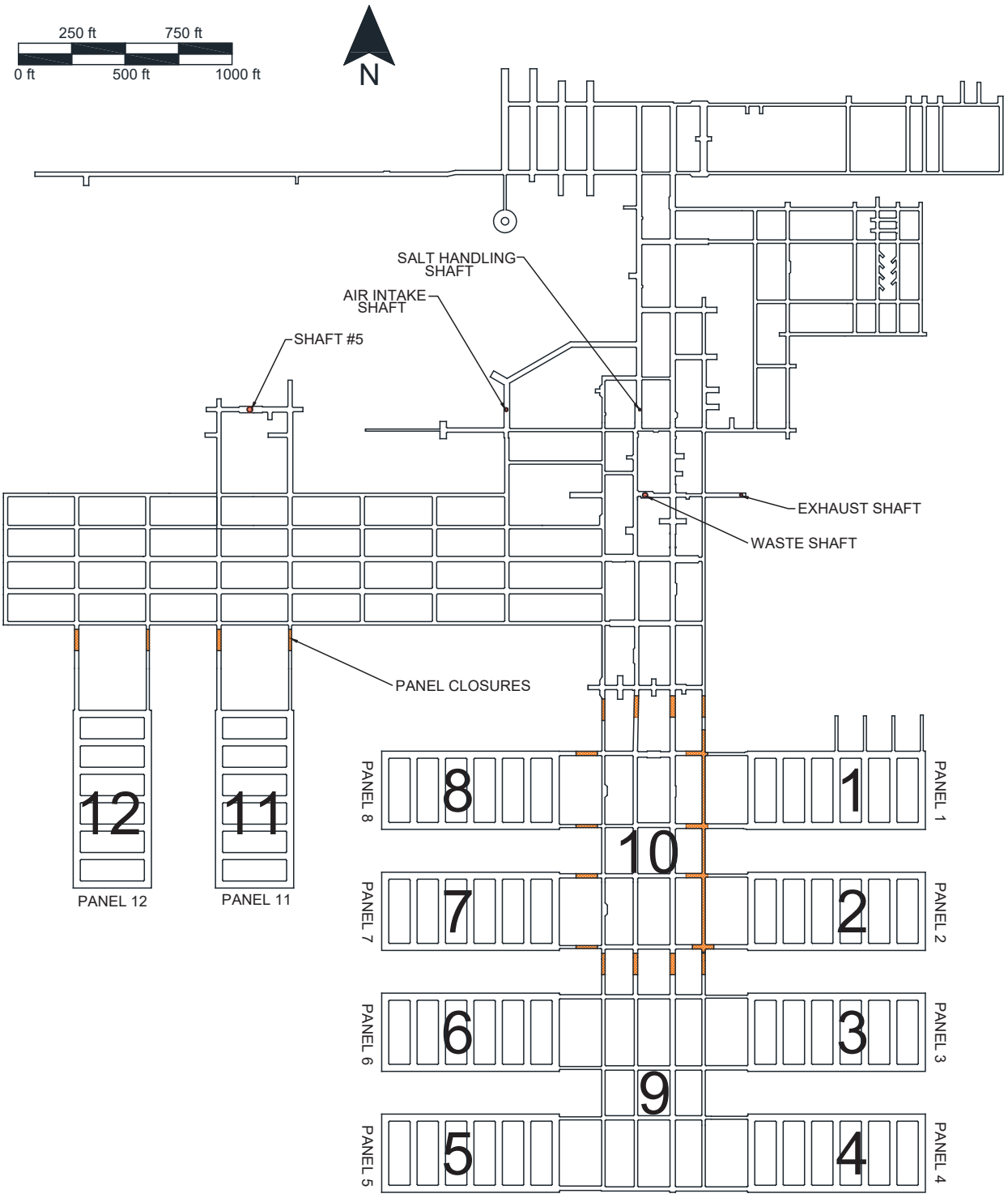

Figure 1. Interim State Repository Layout

Information Only

2.2 Parameters Related to Repository Dimensions

The repository design (Section 2.1) requires changes to several parameters describing repository dimensions. Brunell (2025) revises four parameters to align with the dimensions used in the development of the Salado flow and transport grid (Section 2.3). The parameters include:

- the waste storage volume (REFCON:VREPOS).
- the area of the berm placed over the waste panels (REFCON:ABERM).
- the area allocated for contact-handled (CH) waste disposal (REFCON:AREA_CH).
- the fraction of the repository volume occupied by CH waste (REFCON:FVW).

Although not listed in AP-214 as an anticipated change (Hansen et al. 2025), the area for emplaced remote-handled (RH) waste (REFCON:AREA_RH) is revised by King (2025b) due to the reduced inventory volume used in the CRA26_IS PA calculation (see Section 2.2). The updated values are provided in Table 1, with REFCON:VREPOS being the only parameter in this list that may impact the Salado flow results.

Table 1. Changed Repository Parameters

Material	Property	RPPCR Value	CRA-2026 IS Value	Units
REFCON	VREPOS	853,284.89	560,722.29	m^3
REFCON	ABERM	1,268,303	750,000	m^2
REFCON	AREA_CH	216,952	141,511	m^2
REFCON	FVW	0.197	0.279	-
REFCON	AREA_RH	15,760	3,528	m^2

2.3 Updates to the Salado Flow and Transport Computational Grid

Dimensions in the computational grid for the Salado flow (BRAGFLO) and transport (NUTS) calculation are changed to be consistent with the interim state repository dimensions (Section 2.1). Day (2025a) modifies the computational grid based on as-built excavation footprint dimensions within the existing repository, plans for future excavations, and the planned change for alternative panel closure locations for Panels 1 and 2 (Knerr 2020). The Salado flow and transport computational grid is shown in Figure 2.

Information Only

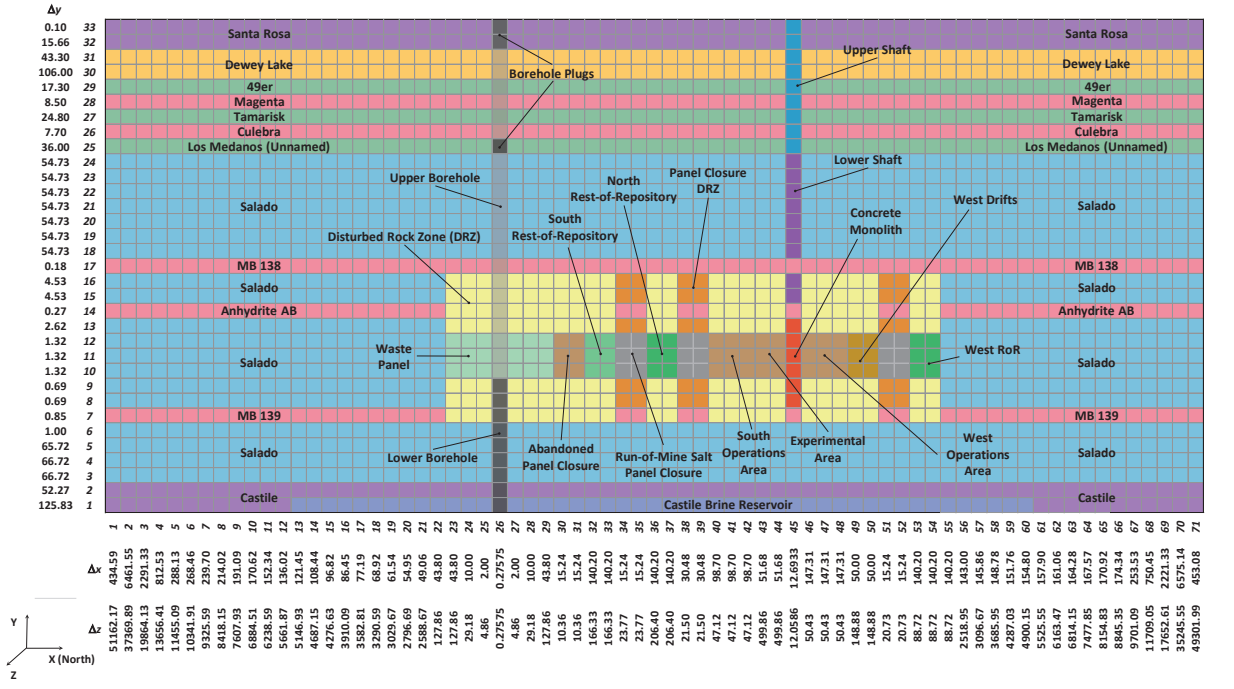

Figure 2. CRA26_IS Salado Flow and Transport Computational Grid

2.4 Waste Inventory

The LWA establishes a statutory limit on the volume of waste that can be disposed of in the WIPP repository, set at 175,564 m^3 (6,200,000 ft^3). Current assessments indicate that the interim state repository will accommodate less waste than the LWA volume. Ward (2025) provided an assessment of the projected waste storage capacity at 157,831.92 m^3, which includes 156,247.12 m^3 of Contact-Handled (CH) waste and 1,584.80 m^3 of Remote-Handled (RH) waste. Based on information collected up to December 31, 2023, the Interim State Performance Assessment Inventory Report – 2024 (ISPAIR-2024; Van Soest 2025) offers an inventory estimate scaled to the waste volume specified by Ward. Kicker (2025) conducted a screening analysis of the inventory estimates for the ISPAIR-2024 to define the inventory-related input parameters for the PA calculations.

2.5 Baseline Actinide Solubilities

Thermodynamic calculations are used to compute the baseline solubilities for actinides in the +III, +IV, and +V oxidation states in GWB and ERDA-6 brines for five multiples of the minimum brine volume for a DBR event. These baseline solubility calculations account for inventory components and thus are updated to be consistent with inventory estimates. Domski (2025b) reports the baseline solubility values based on the CRA26_IS inventory.

Currently there is no thermodynamic model for WIPP actinides in the +VI oxidation state. The Los Alamos National Laboratory Actinide Chemistry and Repository Science Program (LANL-

Information Only

ACRSP) has performed experimental investigations on U(VI) solubility under WIPP-relevant conditions. Based on this experimental work, Kaplan et al. (2025) recommends a solubility of 3×10^{-6} M for actinides in the +VI oxidation state in both Salado and Castile brines.

2.6 Solubility Uncertainty Distributions

Actinide solubility uncertainty distributions, which are independent of the repository inventory, are updated for CRA-2026, as documented in Domski (2025a). A literature review was conducted to identify relevant studies published prior to the CRA-2026 cutoff date. Based on this review, the uncertainty distribution for +III actinide solubilities (SOLMOD3:SOLVAR) is updated. No new literature was found for +IV actinide solubilities; therefore, no update to the +IV solubility uncertainty distribution is made.

2.7 Colloidal Enhancement Parameters

Based on updates to the thermodynamic model and baseline solubility values, Mariner (2025) reevaluated the proportionality constant for humic colloids. Mariner recommends updated values for radionuclides in the +III oxidation state for both Castile and Salado brines (PHUMOX3:PHUMCIM and PHUMOX3:PHUMSIM). Mariner recommends no change to values for radionuclides in the +IV oxidation state.

In previous WIPP PA calculations, microbial colloid enhancement parameters (PROPMIC and CAPMIC) have been specified for each element (parameter materials AM, NP, PU, TH, and U). For the CRA-2026 PA, the microbial enhancement parameters have been specified for each element-oxidation state (materials AM+3, NP+4, NP+5, PU+3, PU+4, U+4, and U+6), in order to more closely align to the experimental data used to derive the parameter values. Kaplan et al. (2025) recommends the microbial colloid parameter values for the CRA-2026 PA.

2.8 MgO Hydration Parameters

The rate of hydration of MgO to form brucite, $Mg(OH)_2$, in the Salado flow model is specified for humid (WAS_AREA:BRUCITEH), Castile brine inundated (WAS_AREA:BRUCITEC), and Salado brine inundated (WAS_AREA:BRUCITES) conditions. Although changes to the MgO hydration rate parameters were not anticipated in AP-214 (Hansen et al. 2025), Nemer (2025) recommends new parameter distributions for the Castile and Salado brine inundated conditions. King (2025a) redefines the recommended distributions to be compatible with the WIPP PA code LHS.

2.9 Lower Bound on Capillary Pressure in the Anhydrite Marker Beds

To improve numerical stability of the Salado flow model when using the modified van Genuchten-Parker capillary pressure function in the anhydrite marker beds, the PA code BRAGFLO was updated to Version 8.00 (WIPP PA 2025) to implement a new capillary pressure model which

Information Only

incorporates a lower bound on the capillary pressure. This lower bound is applied when brine saturations exceed one minus the residual gas saturation. Day (2025b) sets the lower bound on capillary pressure to 1 atm (101325 Pa), with the PO_MIN property of the S_MB139, S_ANH_AB, and S_MB138 materials, and applied the new capillary pressure model by setting the CAP_MOD property to 6 for the same materials.

2.10 Porosity-Permeability Parameter Distribution

King (2025a) redefines the distribution for the parameter representing the relationship between porosity and permeability in a run-of-mine salt panel closure system during the secondary time duration (PCS_T2:POR2PERM). Initially defined as a truncated normal distribution, this parameter is revised, along with the MgO hydration parameters (Section 2.8), to a cumulative distribution characterized by discrete data points. This change constitutes a deviation from AP-214 (Hansen et al. 2025).

2.11 Parameters Not Updated as Anticipated in Analysis Plan AP-214

AP-214 (Hansen et al. 2025) indicates that several parameters were expected to be updated for CRA-2026. Specifically, the parameter specifying the likelihood of low or high oxidation state for an actinide (property OXCUTOFF for materials NP, PU, and U) and the parameters related to mineral and intrinsic colloids (properties CONCMIN and CONCINT for materials AM, NP, PU, TH, and U) were anticipated to undergo revisions. Kaplan et al. (2025) re-examines the basis for these parameter values and recommends the continued use of the RPPCR values. As a result, no changes were made to these parameters for CRA-2026.

Information Only

3.0 CONCEPTUAL APPROACH FOR THE CRA-2026

The conceptual approach for DBR for the CRA26_IS analysis is the same as for the RPPCR and is described in this section.

If the WIPP repository were to be penetrated by a borehole while under conditions of sufficient repository brine pressure and saturation, brine could migrate up through the intruding borehole to reach the land surface. Such an event is defined as a DBR. As with previous WIPP PAs, the BRAGFLO DBR analysis uses the BRAGFLO code to numerically evaluate the volumetric flux of brine that enters the borehole over the duration of the release using the well deliverability equations (Mattax and Dalton 1990):

$$\text{DBR volume} = \int_0^{t_e} q_b(t)\, dt = \int_0^{t_e} J_b \left[p_b(t) - p_{wf}\right] dt \quad . \tag{1}$$

In equation (1):

t elapsed time since drilling intrusion [s];

t_e duration of the DBR event [s];

$q_b(t)$ volumetric flux [m^3/s] of brine into the intrusion as a function of time;

J_b well productivity index [m^3/(Pa·s)];

$p_b(t)$ brine pressure [Pa] calculated by BRAGFLO at the location of the intrusion; and

p_{wf} flowing bottom-hole pressure [Pa].

The duration of the DBR event (t_e) is between 3 and 4.5 days. After 3 days, if at any time the gas flowrate in the borehole falls below the gas cut-off rate of 100 mscf/day (2832 m^3/day) it is assumed the well would be cased and the DBR event ends at that time. If the gas flow rate remains above the cut-off rate, it is assumed the well could be brought under control after 4.5 days, ending the DBR event (Kirkes 2007).

Values for the flowing bottom-hole pressure, p_{wf}, were previously tabulated through an iterative calculation assuming equilibrium with atmospheric pressure at the ground surface for a range of repository pressures and saturations. Curve fit functions of these tables were then created for different flow regimes (all-brine, brine-dominated, and gas-dominated). The flowing bottom-hole pressure is calculated from these look-up table fit functions (Stoelzel and O'Brien 1996).

The well productivity index, J_b, is a measure of how readily brine can enter the well. In a radial drainage area with uniform saturation, it can be determined from Darcy's law (Chappelear and Williamson 1981):

$$J_b = \frac{2\pi k k_r h}{\mu[ln(r_e/r_w)+s-0.5]} \quad . \tag{2}$$

In equation (2):

k intrinsic permeability of the waste [m^2];

k_r relative permeability of the waste to brine [--];

Information Only

h height of the crushed panel [m];

μ brine viscosity [Pa·s];

r_e effective drainage radius of the intruded cell [m];

r_w radius of the wellbore [m]; and

s skin factor [--].

Relative permeability is computed using the model of Brooks and Corey (1964) given by $k_r = S_e^{3+2/\lambda}$ where λ is the pore distribution parameter, $S_e = (S_b - S_{br})/(1 - S_{br})$ is the effective brine saturation, S_b is the brine saturation at the time of the intrusion, and S_{br} is the residual brine saturation. The crushed panel height is defined as $h = h_i(1 - \phi_i)/(1 - \phi)$, where h_i and ϕ_i are the initial height and porosity of the waste and ϕ is the volume-averaged porosity of the waste at the time of intrusion (Helton et al. 1998). The effective drainage radius is defined by $r_e = \sqrt{\Delta x \Delta y/\pi}$, where Δx and Δy are the dimensions of the grid cell containing the well (see Figure 3). The wellbore radius is fixed at 0.1556 m, based on the assumption of a 12.25 in. drill bit diameter. Lastly, as described by Helton et al. 1998, skin factor s is used to incorporate flow stimulation caused by spallings release: $s = -ln\left[\sqrt{\frac{V_i}{\pi h_i}}/r_w\right]$, where V_i is the uncompacted volume of spallings material. Note that J_b is constant for a particular drilling intrusion and that in Equation 1 only brine pressure $p_b(t)$ is a function of time.

The PA parameter values used to compute the DBR volumes are summarized in Table 2. All except the residual brine saturation in the waste are constant.

Table 2. Summary of PA Parameters Used to Compute DBR Volumes

PA Parameter	Description	Value
WAS_AREA:PRMX_LOG[a]	Intrinsic permeability of the waste (k)	2.4×10^{-13} m^2
WAS_AREA:PORE_DIS	Brooks-Corey pore distribution parameter (λ)	2.89
WAS_AREA:SAT_RBRN	Residual brine saturation in the waste (S_{br})	Uniform distribution Max: 0.552 Mean 0.276 Min 0.000
BRINESAL:VISCO	Brine dynamic viscosity (μ)	0.0021 Pa·s
BOREHOLE:DIAMMOD	Drill bit diameter ($2 \times r_w$)	0.311 m
BLOWOUT:HREPO	Initial waste panel height (h_i)	3.96 m
BLOWOUT:MINFLOW	Minimum duration of DBR	3 days
BLOWOUT:MAXFLOW	Maximum duration of DBR	4.5 days
BLOWOUT:GAS_MIN	Gas cut-off rate	2832 m^3/day

[a]-The definition of this parameter in the Parameter Database is the logarithm of the intrinsic permeability and has a value of -12.6198.

Information Only

As defined for WIPP PA, minimum pressure and saturation conditions must exist within the waste panel for brine to flow to the surface during an intrusion and produce a DBR. Pressure in the intruded waste panel must be great enough to overcome the static pressure exerted by a column of drilling fluid at the repository depth, assumed to be equal to 8 megapascals (MPa). Brine saturation in the intruded waste panel must be above the residual brine saturation of the waste, that is, the brine must be mobile.

3.1 Model Geometry

The BRAGFLO_DBR model explicitly represents the vicinity of the waste panels, including specific repository features like individual panels and panel closures, in a 2-dimensional rectilinear grid. Like the BRAGFLO Salado Model (Day and King 2025), the grid dips 1º to the south.

The DBR numerical grid and material map used in the CRA26_IS PA is the same as that used in the RPPCR calculations and is shown in Figure 3. The reduced repository area included in the CRA26_IS representation of the WIPP in Salado flow calculations did not result in a change to the DBR grid representation, as it already adequately considers the connections between the Salado flow results and DBR initial conditions for each of the waste regions. With the short duration of DBR simulations, there is very little communication across panel closures; therefore, there is not a need to have an explicit representation of repository volume outside of the panel closures containing the intrusion locations. Four drilling locations are considered in the CRA26_IS PA: “U” (for upper, since it is up-dip), “M” (for middle), and “L” (for lower, since it is down-dip), and “O” (for other). These intrusion locations are shown in Figure 3.

Some of the DBR volume calculations are for a drilling intrusion preceded by an E1 intrusion in either the same or a different waste panel. An E1 intrusion is a borehole that intersects the repository and then continues down to penetrate a hypothetical brine reservoir. The effects of a prior E1 intrusion are incorporated into the calculations by specifying pressure at a boundary condition well. The location of the boundary condition well is denoted by the red dot in Figure 3. Properties of the boundary condition well depend on the amount of time that has elapsed since the previous E1 intrusion occurred, as this determines whether the borehole between the repository and the brine reservoir is open, contains fill, or is closed due to salt creep. Formulas for determining the boundary well pressure under the different borehole conditions are given in Helton et al. (1998).

Information Only

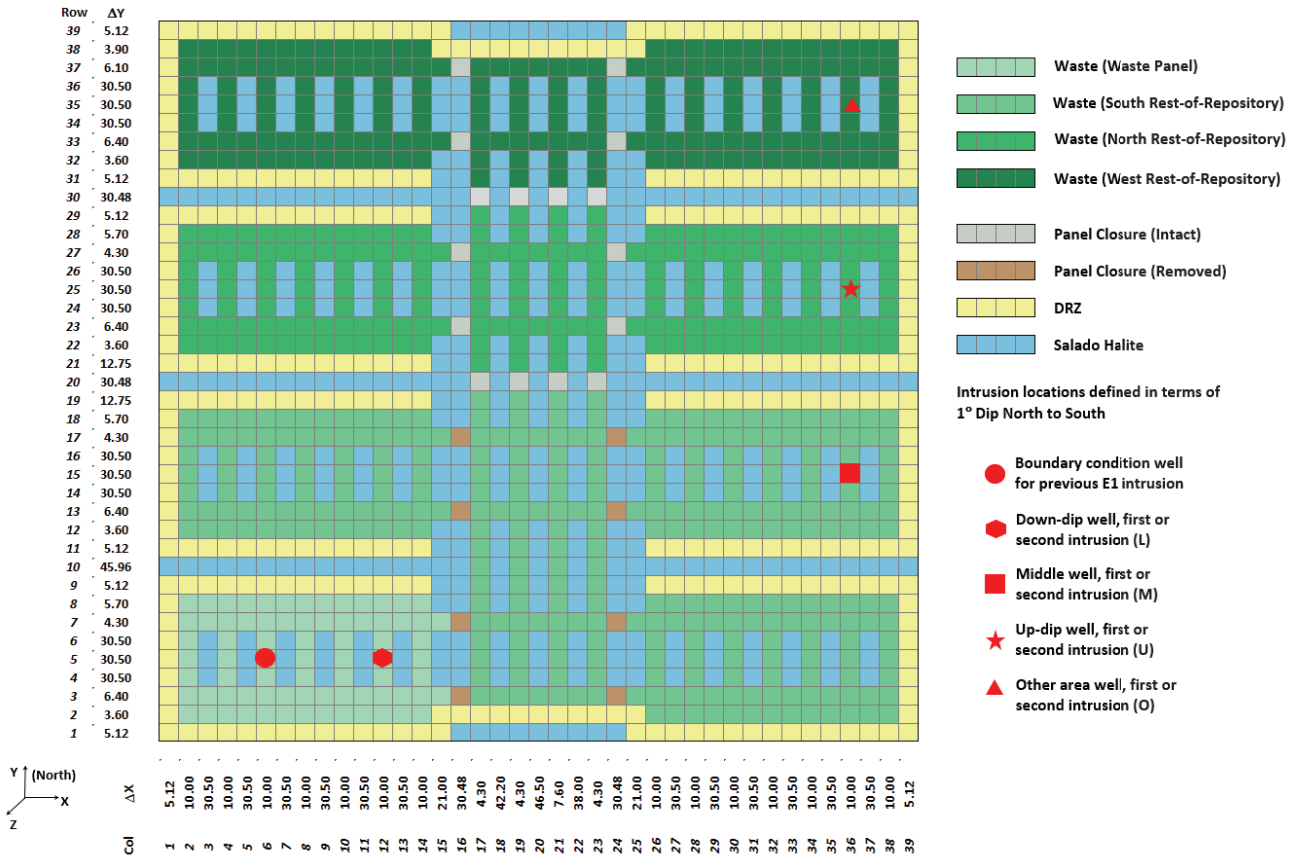

Figure 3. CRA26_IS and RPPCR DBR Grid with Simulated Intrusion Locations

3.2 Initial Conditions

Brine pressures and brine saturations calculated during the BRAGFLO Salado flow simulations (Day and King 2025) are volume-averaged and used as initial conditions in the DBR simulations. Figure 4 illustrates the method used to transfer initial conditions in the waste for the CRA26_IS. The BRAGFLO grid aggregates waste panels into four waste-bearing regions: Waste Panel, South Rest-of-Repository, North Rest-of-Repository, and West Rest-of-Repository (King 2023). In Figure 4, these regions are denoted Waste Panel, SRoR, NRoR and WRoR, respectively. At the time of the intrusion, the volume-averaged pressure and saturation from the four waste-filled regions in the BRAGFLO grid are used as the initial pressure and saturation for corresponding waste regions in the DBR grid. Consistent with the designations L, M, U and O for the intrusion locations, the DBR grid waste regions will be referred to as Lower, Middle, Upper, and Other. As indicated in Figure 4, conditions in the BRAGFLO Waste Panel map to the Lower waste region in the DBR grid; likewise, BRAGFLO SRoR conditions map to the Middle DBR region, NRoR to the Upper DBR region, and WRoR to the Other DBR region. Note that pressure and saturation are allowed to change during the DBR volume calculations.

Information Only

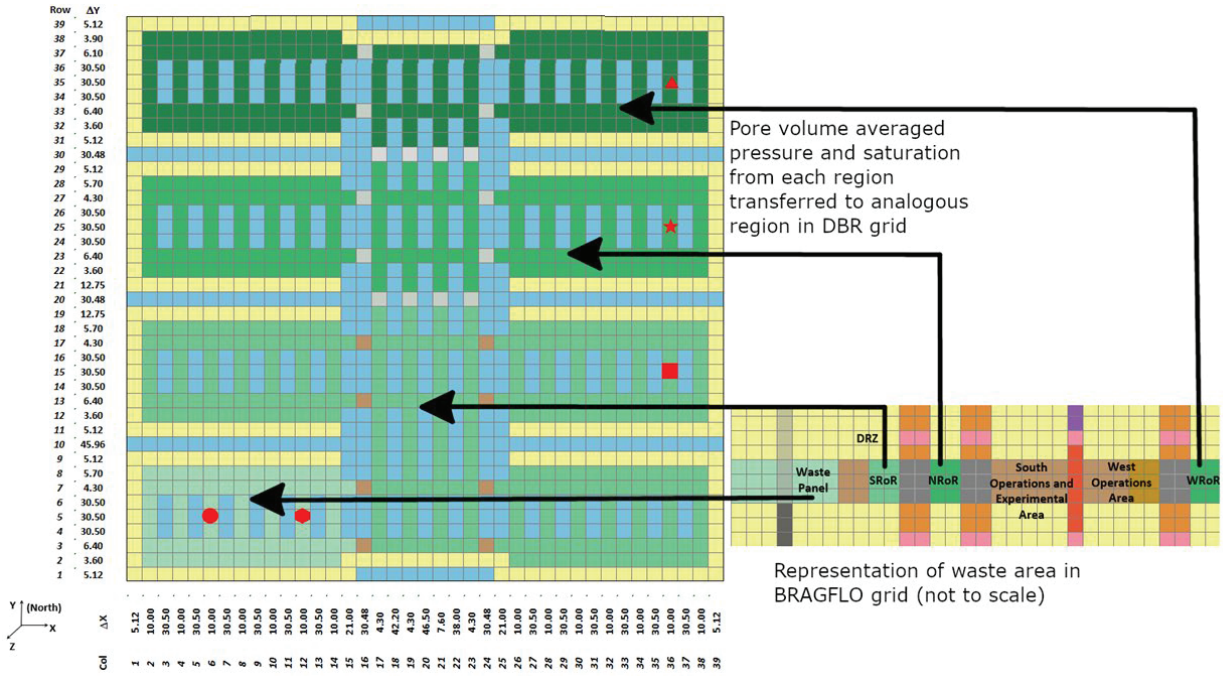

Figure 4. Regions Used to Transfer Initial Pressure and Saturation from the BRAGFLO Salado Grid to the DBR Grid

Information Only

4.0 DBR METHODOLOGY

This section provides an overview of the methodology used in the CRA26_IS DBR volume calculations, including the modeled scenarios and run control narrative. The methodology is the same as used in the RPPCR DBR volume calculations.

4.1 Modeled Scenarios

In performing DBR volume calculations, five of the BRAGLFO Salado flow model scenarios, S1-BF to S5-BF, are used to set the initial conditions for the DBR volume calculations at the time of intrusion. As described by Day and King (2025), the five BRAGFLO Salado flow scenarios capture the long-term behavior of the repository under three different conditions: undisturbed (E0); intersected by a borehole that continues down to a hypothetical pressurized brine reservoir below the repository (E1); and intersected by a borehole that does not intersect pressurized regions below the repository (E2). DBR volume calculations map the resulting BRAGFLO pressure and saturation conditions at a suite of intrusion times onto the DBR model grid and simulate flow to the intrusion. The scenarios and intrusion times used for the RPPCR, presented in Table 3, are the same as those used for the RPPCR. There are a total of 104 combinations, or DBR simulations, for each parameter vector.

Table 3. DBR Scenarios

Scenario	Description
S1-DBR	Initially undisturbed repository (E0 conditions). Intrusion at the L, M, U, or O location at 100; 350; 1,000; 3,000; 5,000; or 10,000 years: 24 combinations.
S2-DBR	Initial E1 intrusion at 350 years followed by a second intrusion at the L, M, U, or O location at 550; 750; 2,000; 4,000; or 10,000 years: 20 combinations.
S3-DBR	Initial E1 intrusion at 1,000 years followed by a second intrusion at the L, M, U, or O location at 1,200; 1,400; 3,000; 5,000; or 10,000 years: 20 combinations.
S4-DBR	Initial E2 intrusion at 350 years followed by a second intrusion at the L, M, U, or O location at 550; 750; 2,000; 4,000; or 10,000 years: 20 combinations.
S5-DBR	Initial E2 intrusion at 1,000 years followed by a second intrusion at the L, M, U, or O location at 1,200; 1,400; 3,000; 5,000; or 10,000 years: 20 combinations.

Information Only

4.2 Code Execution and Run Control

A flow diagram that illustrates the execution order for the DBR model is provided in Figure 5. A full description of the run control for the RPPCR analysis, including names and locations of input and output files, can be found in Long (2025).

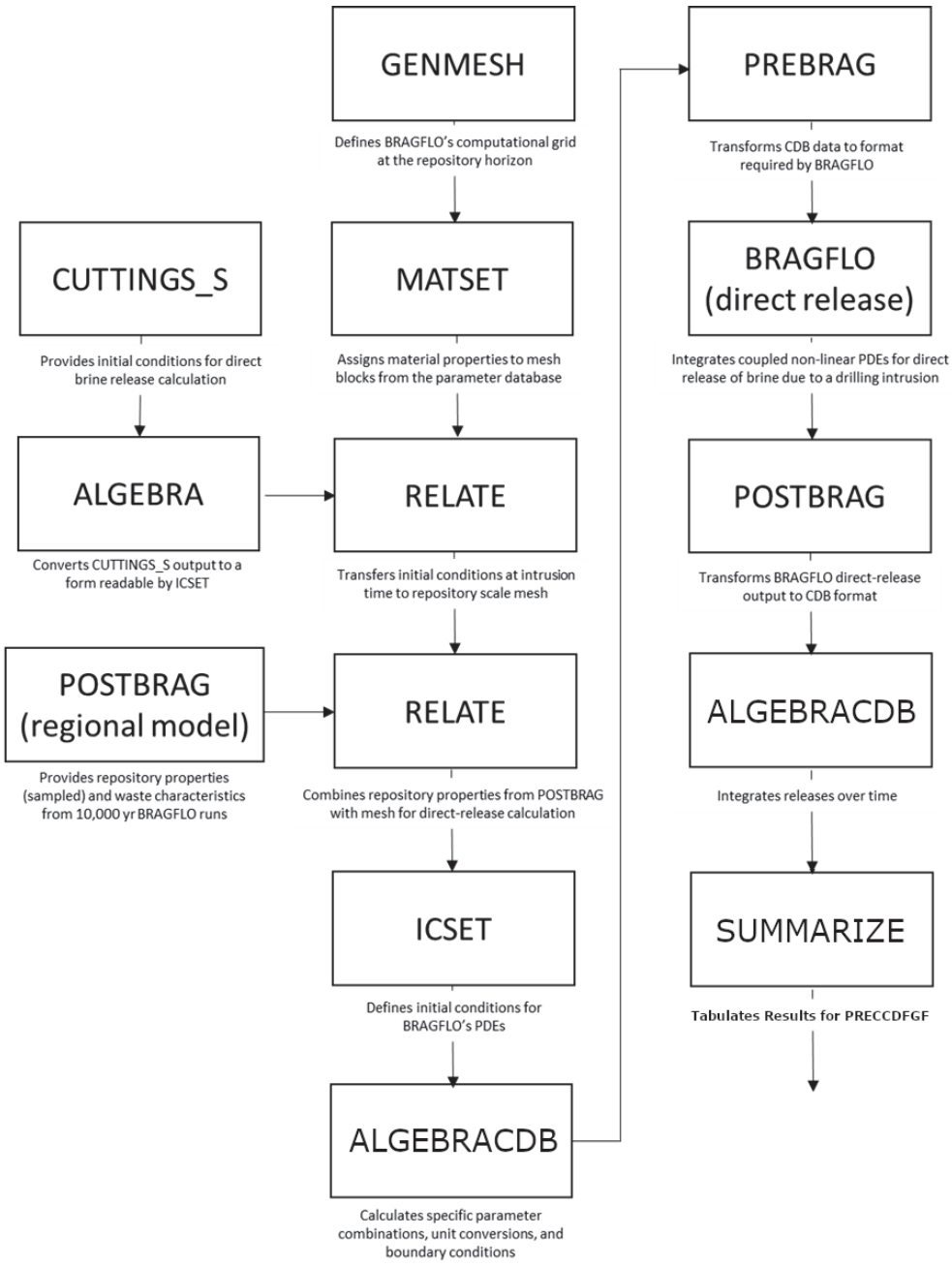

Figure 5. DBR Run Control Diagram

Information Only

5.0 RESULTS

The DBR volume calculation results for the CRA26_IS are presented in this section and compared to results from the RPPCR (Docherty and King 2023). In WIPP PA, a replicate consists of 100 calculated realizations (vectors). Results for three replicates were calculated for the CRA26_IS and RPPCR analyses. Only results from Replicate 1, including means, statistics, and sensitivity analyses, will be presented in this section.

Results from all scenarios are summarized below. Results are then further examined for scenarios S1-DBR, S2-DBR, and S4-DBR. Results from S3-DBR and S5-DBR are not examined individually because the only difference between them and S2-DBR and S4-DBR, respectively, is in the timing of drilling intrusions.

Summary statistics and plots were generated with Python, an open-source software package. The average DBR volume is calculated by the sum of DBR volumes divided by the total number of simulations. The DBR volume data were obtained from the output variable BRIN_REL, which is calculated in the ALGEBRACDB post-processing step and tabulated with PA code SUMMARIZE. For consistency with previous analyses, in calculating average non-zero DBR volumes and rates, non-zero volumes are defined as volumes that are greater than 10^{-7} m^3.

In addition to tables, many of the results are presented as boxplots, which graphically depict the distribution of the data by drawing boxes around the 25th (Q_{25}) and 75th (Q_{75}) percentiles of the distribution with a bisecting line at the median. The box whiskers extend out from the box to either an additional 1.5*(Q_{75} - Q_{25}) or to the full range of the data, whichever is closer to the median. Datapoints outside of the whisker range are marked on the plot with black diamonds. The mean value is marked with a white square on top of the box and whisker plot. Note that intrusion time is treated categorically when used as an axis on the boxplots in this section.

5.1 Summary

Mean brine releases, fraction of simulations with non-zero releases, and mean of non-zero brine releases are summarized in Table 4. The number of non-zero brine releases is plotted in Figure 6 by brine release volume, and the distribution of non-zero brine release volumes is plotted in Figure 7. Figure 8 shows the distribution of non-zero release volumes broken down by scenario, and Figure 9 shows the number of non-zero releases by scenario.

Making an overall comparison of DBR volumes for the RPPCR and the CRA26_IS:

(i) The number of non-zero DBR volumes decreased for the CRA26_IS across all scenarios (Figure 9).
(ii) The CRA26_IS saw small magnitude releases decrease in frequency (Figure 6), while large magnitude releases (greater than 50 m^3) increased slightly in frequency (though they represent a very small fraction of release events) (Figure 7).
(iii) Mean and median non-zero release volumes all decreased for the CRA26_IS, while maximum non-zero release volumes increased (Figure 7). Overall, the mean non-zero release volume decreased by about 10% (Table 4).

Information Only

(iv) For the CRA26_IS, mean non-zero release volumes are decreased for scenarios S1-DBR, S2-DBR, and S3-DBR, but increased for the other two scenarios (Figure 8). Median release volumes are decreased for all scenarios except S4-DBR. Maximum release volumes are increased for all scenarios except S1-DBR.

(v) For both the RPPCR and the CRA26_IS, the largest fraction of non-zero DBR volumes occurs at the L intrusion location and decreases as the intrusion location moves to the north, that is, up dip to the M, U, and O locations (Table 4). The largest mean non-zero release volume also occurs at the L intrusion location and decreases as the intrusion location moves to the north to the M intrusion location, but then increases for the U intrusion location, and finally decreases to the lowest volume for the O intrusion location.

(vi) Releases from the O intrusion location contribute to RPPCR and CRA26_IS DBR volumes; however, O intrusion releases are less frequent and mean volumes are smaller compared to the L, M and U intrusion locations (Table 4).

As described by Day and King (2025), the CRA26_IS Salado flow results show a decrease in mean brine pressures for scenarios without an E1 intrusion and an increase in mean brine pressures for scenarios with an E1 intrusion (except for the westernmost waste areas). Additionally, there is an observed decrease in brine saturation. The combination of these effects could lead to mixed impacts on the number of non-zero DBR volumes across scenarios. Day and King (2025) also points out that maximum brine pressure for any individual vector in Replicate 1 is generally greater in the CRA26_IS and there is a substantial decrease in brine saturation; these are effects that could also lead to mixed impacts on the magnitudes of the largest DBR volumes.

Comparing CRA26_IS and RPPCR DBR volumes at individual intrusion locations (in Table 4, rows directly beneath the “All Scenarios” label), DBR volumes for all intrusion locations follow the overall trend of a decreased frequency of non-zero DBR volumes and with decreased mean non-zero release volumes in the CRA26_IS. In both analyses, DBR volumes from the L location have the greatest frequency and mean non-zero release volume. DBR volumes at the M location have decreased frequency and mean non-zero release volumes compared to the L location, but the mean non-zero release volumes are also lower compared to the U intrusion location for Replicate 1 in both analyses. In Docherty and King (2023), the comparison of DBR volumes was made between the RPPCR and CRA19 analyses across all three replicates, rather than on a replicate-by-replicate basis; that comparison showed a consistent overall trend of decreased mean DBR volumes moving north from the L location to the M, U, and O locations.

Scenarios with an E1 intrusion (S2-DBR and S3-DBR) have a decreased frequency of non-zero DBR volumes in the CRA26_IS; additionally, mean non-zero release volumes in the CRA26_IS are decreased by about 20-25% compared those in the RPPCR (Table 4). The decrease in mean non-zero release volumes can be attributed to reduced brine saturation for scenarios with E1 intrusion, despite increased brine pressures (Day and King 2025) and despite the observed increase in the number of large magnitude releases (Figure 7).

Scenarios without an E1 intrusion (S1-DBR, S4-DBR and S5-DBR) saw the frequency of non-zero DBR volumes also decrease in the CRA26_IS, while mean non-zero releases were reduced by about 20% for S1-DBR and increased by about 10-20% for the other two scenarios (Table 4).

Information Only

The decreased frequency in non-zero DBR volumes can be attributed to decreased brine saturation, as well as decreased mean pressure for scenarios without an E1 intrusion (Day and King 2025). The increased mean DBR volumes for scenarios S4-DBR and S5-DBR can be attributed to increased maximum pressures in CRA26_IS.

Information Only

Table 4. DBR Volume Summary, Replicate 1

Intrusion Location	Mean Brine Released (m^3)		Fraction of Simulations with Non-Zero Releases		Mean of Non-Zero Brine Releases (m^3)	
	RPPCR	CRA26_IS	RPPCR	CRA26_IS	RPPCR	CRA26_IS
S1-DBR	**0.67**	**0.30**	**8.96%**	**5.04%**	**7.48**	**6.05**
L	1.77	0.78	15.17%	9.67%	11.67	8.11
M	0.34	0.20	6.67%	3.67%	5.13	5.53
U	0.42	0.19	8.33%	4.83%	5.02	3.87
O	0.15	0.05	5.67%	2.00%	2.67	2.28
S2-DBR	**2.24**	**1.32**	**37.70%**	**27.75%**	**5.94**	**4.77**
L	5.73	3.66	74.60%	62.40%	7.67	5.87
M	2.45	1.20	55.60%	39.20%	4.41	3.06
U	0.59	0.33	13.80%	6.60%	4.25	5.06
O	0.19	0.10	6.80%	2.80%	2.73	3.57
S3-DBR	**1.40**	**0.69**	**33.30%**	**22.10%**	**4.21**	**3.13**
L	3.73	1.94	68.00%	51.00%	5.48	3.81
M	0.95	0.52	40.00%	27.20%	2.37	1.91
U	0.67	0.25	15.80%	6.80%	4.22	3.68
O	0.26	0.06	9.40%	3.40%	2.80	1.70
S4-DBR	**0.89**	**0.68**	**12.45%**	**7.75%**	**7.18**	**8.79**
L	2.02	1.76	18.40%	15.20%	10.97	11.55
M	0.79	0.52	12.60%	6.80%	6.29	7.65
U	0.58	0.35	12.00%	6.40%	4.86	5.44
O	0.18	0.10	6.80%	2.60%	2.69	3.84
S5-DBR	**1.18**	**0.70**	**14.90%**	**7.90%**	**7.91**	**8.88**
L	2.68	2.07	21.40%	15.20%	12.52	13.61
M	1.00	0.40	14.20%	6.60%	7.04	6.08
U	0.76	0.28	14.60%	6.40%	5.18	4.32
O	0.28	0.06	9.40%	3.40%	2.96	1.79
All Scenarios						
L	**3.13**	**1.99**	**38.58%**	**29.88%**	**8.11**	**6.67**
M	**1.08**	**0.55**	**25.08%**	**16.19%**	**4.30**	**3.43**
U	**0.60**	**0.28**	**12.73%**	**6.15%**	**4.67**	**4.48**
O	**0.21**	**0.07**	**7.54%**	**2.81%**	**2.78**	**2.56**
ALL	**1.25**	**0.72**	**20.98%**	**13.76%**	**5.97**	**5.26**

Information Only

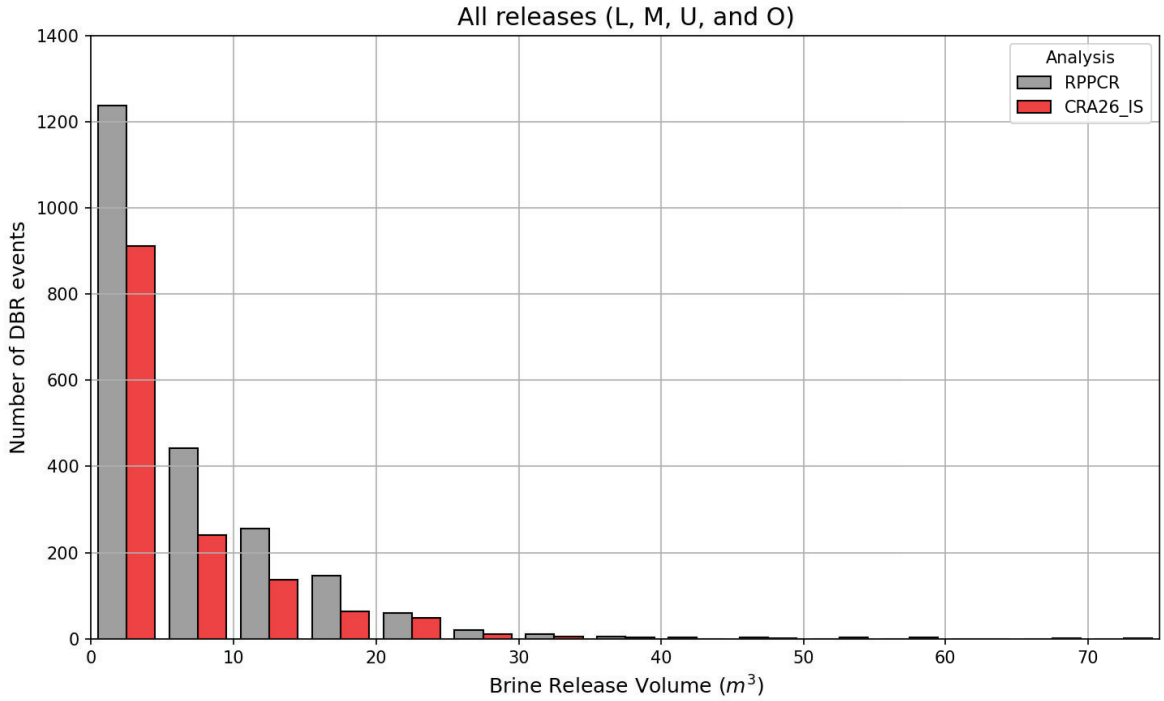

Figure 6. Release Volume Frequency, All Non-Zero Releases, Replicate 1

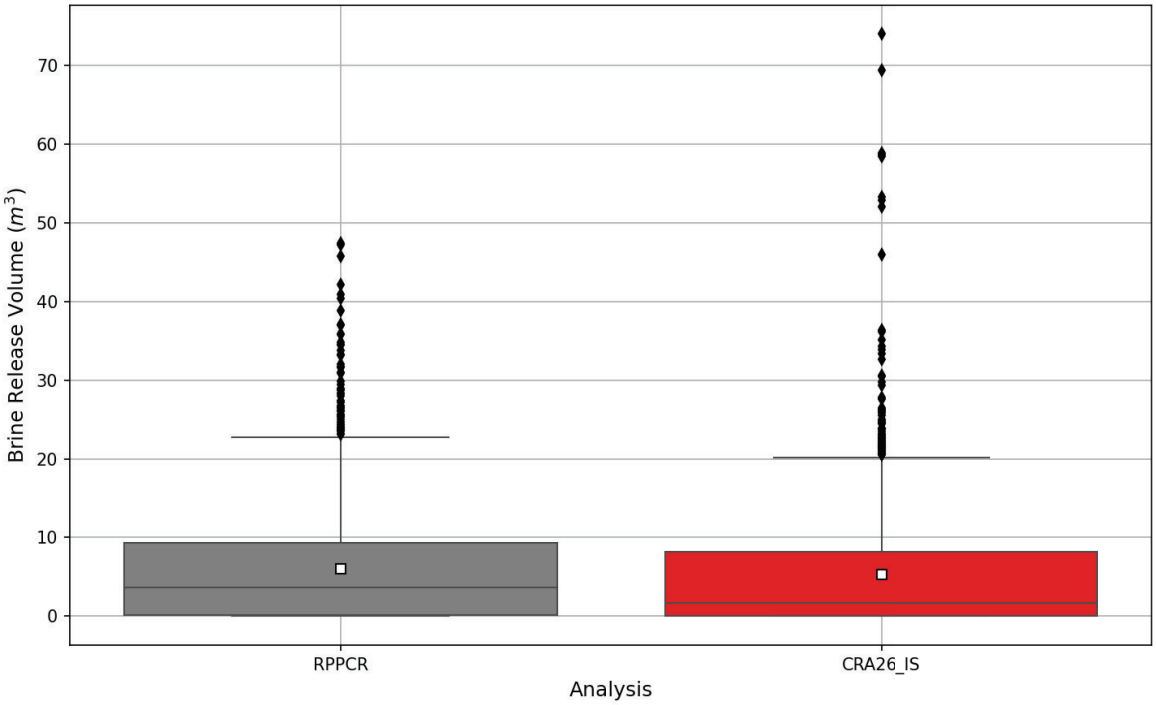

Figure 7. Release Volumes, All Non-Zero Releases, Replicate 1

Information Only

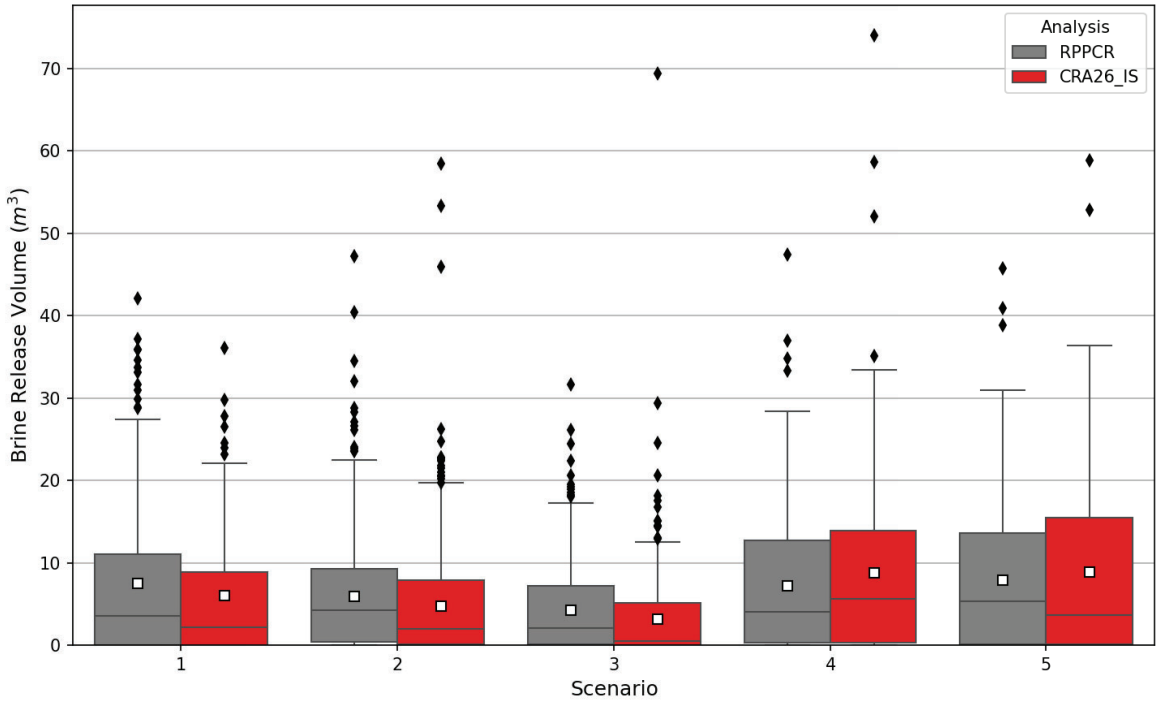

Figure 8. Release Volumes by Scenario, All Non-Zero Releases, Replicate 1

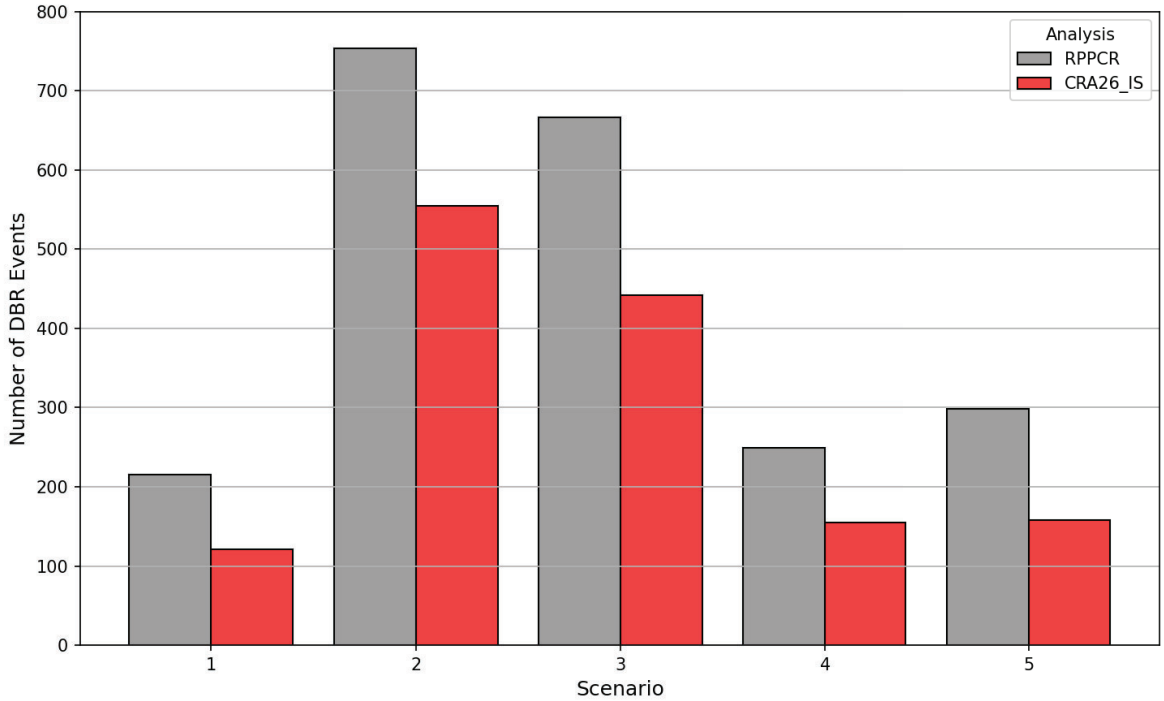

Figure 9. Number of Non-Zero DBR Events by Scenario, Replicate 1

Information Only

5.2 S1-DBR

The S1-DBR scenario models DBR volumes resulting from an intrusion into a previously undisturbed repository (Table 3). Mean brine release volume, fraction of simulations with non-zero releases, and mean volume from non-zero releases are summarized in Table 5. Non-zero release volumes for S1-DBR intrusions are plotted in Figure 10, grouped by intrusion location and time.

Compared to the RPPCR, the S1-DBR fraction of simulations with non-zero releases decreased by about a factor of two for the CRA26_IS, while the mean non-zero release volumes decreased by about 20% (Table 5). The results contrast with other scenarios that do not involve an E1 intrusion (e.g., S4-DBR) where mean non-zero release volumes increased by about 20% (Section 5.4). Also, while these decreases are consistent between Replicates 1 and 3, Replicate 2 results show increases with respect to RPPCR (see Appendix C). For Replicate 2, the fraction of S1-DBR simulations with non-zero releases decreased for all intrusion locations, but the mean of non-zero brine releases increased for all intrusion locations. The observed decrease in non-zero brine volumes after the year 3,000 intrusion is consistent with the strong decrease in mean brine saturations and moderate decrease in mean brine pressures (compared to RPPCR) observed for all waste areas (Day and King 2025).

Information Only

Table 5. S1-DBR Volume Summary, Replicate 1

Intrusion Location and Time (yr)	Mean Brine Released (m^3)		Fraction of Simulations with Non-Zero Releases		Mean of Non-Zero Brine Releases (m^3)	
	RPPCR	CRA26_IS	RPPCR	CRA26_IS	RPPCR	CRA26_IS
L	**1.77**	**0.78**	**15.17%**	**9.67%**	**11.67**	**8.11**
100	0.00	0.00	0.00%	0.00%	-	-
350	0.19	0.28	4.00%	5.00%	4.73	5.51
1,000	2.45	2.20	21.00%	17.00%	11.69	12.92
3,000	3.62	1.55	22.00%	14.00%	16.44	11.10
5,000	2.87	0.29	22.00%	11.00%	13.06	2.64
10,000	1.49	0.39	22.00%	11.00%	6.76	3.53
M	**0.34**	**0.20**	**6.67%**	**3.67%**	**5.13**	**5.53**
100	0.00	0.00	0.00%	0.00%	-	-
350	0.15	0.27	4.00%	5.00%	3.69	5.35
1,000	1.44	0.95	19.00%	12.00%	7.57	7.91
3,000	0.41	0.00	9.00%	3.00%	4.60	0.04
5,000	0.02	0.00	4.00%	1.00%	0.61	0.00
10,000	0.03	0.00	4.00%	1.00%	0.69	0.00
U	**0.42**	**0.19**	**8.33%**	**4.83%**	**5.02**	**3.87**
100	0.00	0.00	0.00%	0.00%	-	-
350	0.05	0.03	1.00%	4.00%	5.19	0.75
1,000	1.34	1.08	18.00%	13.00%	7.42	8.29
3,000	0.69	0.01	15.00%	6.00%	4.60	0.21
5,000	0.21	0.00	9.00%	3.00%	2.32	0.05
10,000	0.22	0.00	7.00%	3.00%	3.21	0.03
O	**0.15**	**0.05**	**5.67%**	**2.00%**	**2.67**	**2.28**
100	0.00	0.00	0.00%	0.00%	-	-
350	0.07	0.00	1.00%	0.00%	6.81	-
1,000	0.50	0.26	9.00%	7.00%	5.55	3.77
3,000	0.28	0.01	9.00%	3.00%	3.08	0.32
5,000	0.05	0.00	8.00%	1.00%	0.60	0.00
10,000	0.01	0.00	7.00%	1.00%	0.21	0.00
S1-DBR	**0.67**	**0.30**	**8.96%**	**5.04%**	**7.48**	**6.05**

Information Only

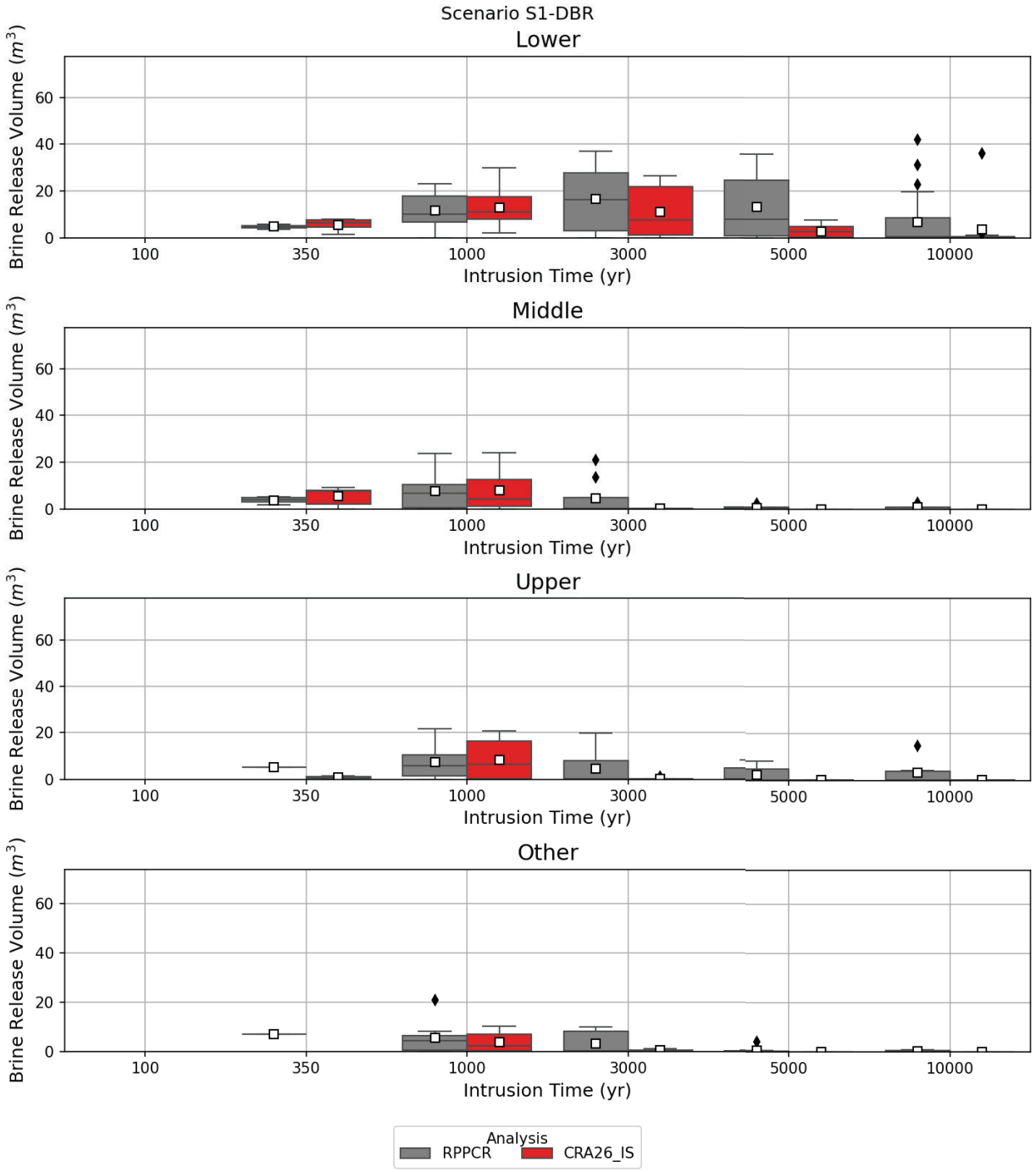

Figure 10. S1-DBR Volumes, All Non-Zero Releases, Replicate 1

Information Only

5.3 S2-DBR

The S2-DBR scenario models DBR volumes resulting from a repository that has been previously intruded by a wellbore that also intersected a pressurized brine pocket in the Castile formation (Table 3). Initial conditions for this scenario are explored in Section 6.1. The CRA26_IS S2-DBR releases are summarized in Table 6, with the RPPCR values shown for comparison. Release volumes for all S2-DBR intrusions are plotted in Figure 11, grouped by intrusion location and time.

For all intrusion locations, the fraction of non-zero releases decreased at all intrusion times. For the L and M intrusion locations, the mean non-zero releases fell by about 20-30%. For U and O intrusion locations, the mean non-zero releases increased by about 20-30% in the CRA26_IS.

The overall reduction in CRA26_IS DBR volumes in the S2-DBR scenario is attributed to reduced brine saturation, despite increased mean brine pressure. A greater number of large magnitude releases due to increased maximum pressure contribute to the observed increase in DBR volumes at the U and O intrusion locations at early times (before year 2,000 intrusions) in the CRA26_IS. Note that maximum release volumes increased for both Replicates 1 and 2, but decreased for Replicate 3 (see Appendix C).

Information Only

Table 6. S2-DBR Volume Summary, Replicate 1

Intrusion Location and Time (yr)	Mean Brine Released (m^3)		Fraction of Simulations with Non-Zero Releases		Mean of Non-Zero Brine Releases (m^3)	
	RPPCR	CRA26_IS	RPPCR	CRA26_IS	RPPCR	CRA26_IS
L	**5.73**	**3.66**	**74.60%**	**62.40%**	**7.67**	**5.87**
550	3.92	2.96	91.00%	87.00%	4.31	3.41
750	6.31	4.83	90.00%	81.00%	7.01	5.96
2000	7.94	5.33	72.00%	57.00%	11.03	9.35
4000	5.70	2.66	62.00%	43.00%	9.20	6.19
10000	4.76	2.53	58.00%	44.00%	8.20	5.76
M	**2.45**	**1.20**	**55.60%**	**39.20%**	**4.41**	**3.06**
550	2.55	2.02	86.00%	80.00%	2.97	2.52
750	3.42	2.15	76.00%	57.00%	4.50	3.76
2000	3.52	1.15	49.00%	35.00%	7.18	3.29
4000	1.62	0.57	37.00%	12.00%	4.37	4.74
10000	1.16	0.12	30.00%	12.00%	3.86	1.01
U	**0.59**	**0.33**	**13.80%**	**6.60%**	**4.25**	**5.06**
550	0.44	0.57	9.00%	9.00%	4.85	6.35
750	0.80	0.92	17.00%	12.00%	4.69	7.68
2000	1.31	0.17	18.00%	8.00%	7.26	2.17
4000	0.13	0.00	13.00%	2.00%	0.98	0.11
10000	0.27	0.00	12.00%	2.00%	2.22	0.02
O	**0.19**	**0.10**	**6.80%**	**2.80%**	**2.73**	**3.57**
550	0.10	0.11	3.00%	3.00%	3.20	3.68
750	0.24	0.27	7.00%	4.00%	3.48	6.73
2000	0.42	0.12	9.00%	4.00%	4.63	3.01
4000	0.15	0.00	7.00%	1.00%	2.13	0.01
10000	0.02	0.00	8.00%	2.00%	0.28	0.00
S2-DBR	**2.24**	**1.32**	**37.70%**	**27.75%**	**5.94**	**4.77**

Information Only

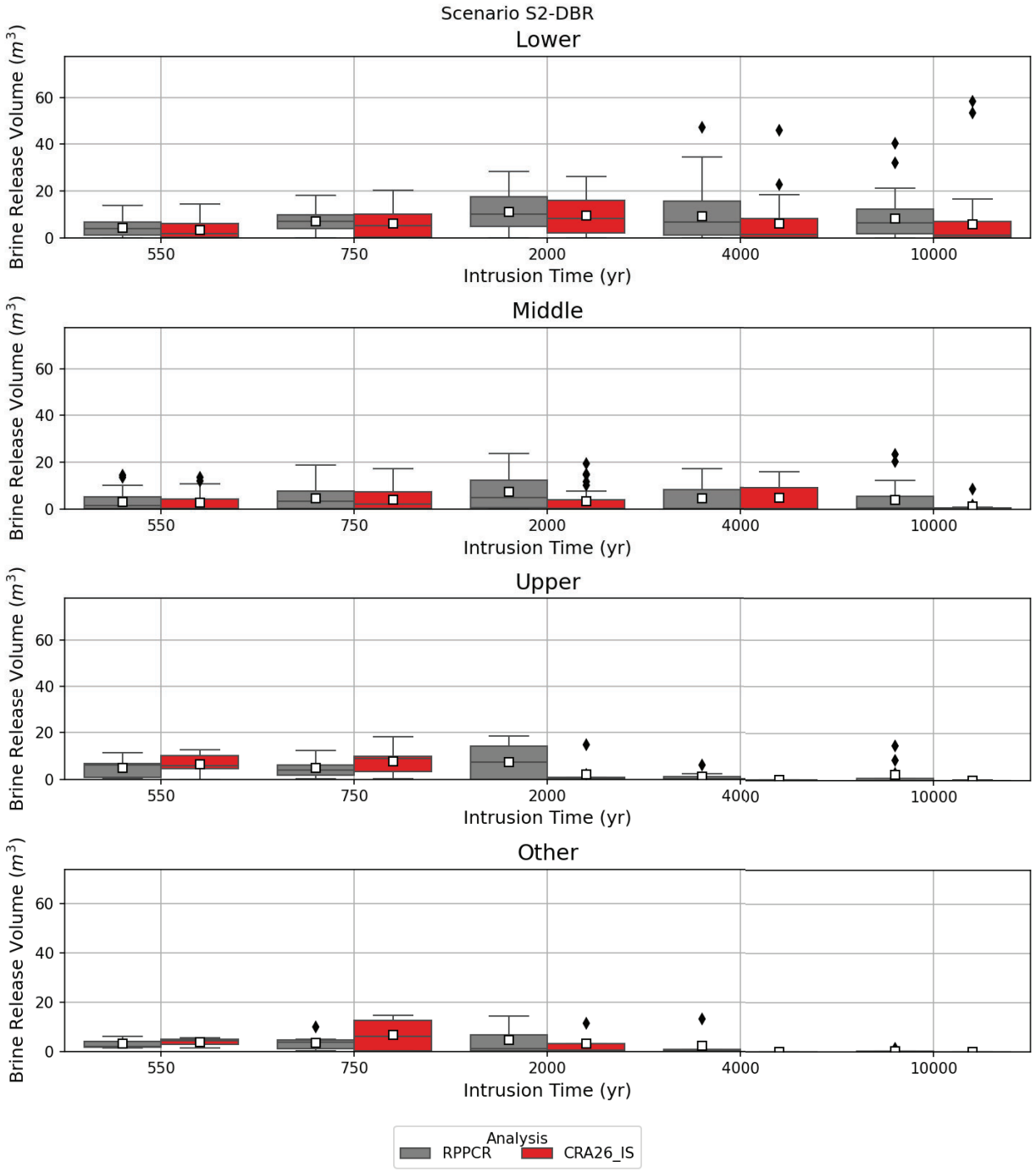

Figure 11. S2-DBR Volumes, All Non-Zero Releases, Replicate 1

Information Only

5.4 S4-DBR

The S4-DBR scenario models DBR volumes resulting from a repository that had been previously intruded by a wellbore that did not intersect a pressurized brine pocket in the Castile formation (Table 3). CRA26_IS S4-DBR release volumes are summarized in Table 7, with RPPCR values for comparison. Release volumes for all S4-DBR intrusions are plotted in Figure 12, grouped by intrusion location and time.

For all intrusion locations, the fraction of non-zero releases were decreased or very similar at all intrusion times. However, the mean non-zero releases increased for all intrusion locations. For the L and M intrusion locations, the mean non-zero releases increased by about 5-20%. For U and O intrusion locations, the mean non-zero releases increased by about 10-40% in the CRA26_IS.

The overall increase in the CRA26_IS DBR volumes in the S4-DBR scenario is observed, despite reduced mean brine pressure and reduced mean brine saturation (Section 6.1). This is possible due to the specific combinations of brine pressure and saturation for a given intrusion. Also, the overall change in DBR volume is relatively small. Note that maximum release volumes increased for both Replicates 1 and 2, but decreased for Replicate 3 (see Appendix C).

Information Only

Table 7. S4-DBR Volume Summary, Replicate 1

Intrusion Location and Time (yr)	Mean Brine Released (m^3)		Fraction of Simulations with Non-Zero Releases		Mean of Non-Zero Brine Releases (m^3)	
	RPPCR	CRA26_IS	RPPCR	CRA26_IS	RPPCR	CRA26_IS
L	**2.02**	**1.76**	**18.40%**	**15.20%**	**10.97**	**11.55**
550	0.92	1.14	12.00%	14.00%	7.68	8.12
750	1.57	1.55	18.00%	16.00%	8.70	9.69
2000	2.79	2.29	20.00%	15.00%	13.93	15.23
4000	2.98	1.96	20.00%	14.00%	14.91	13.99
10000	1.83	1.85	22.00%	17.00%	8.33	10.87
M	**0.79**	**0.52**	**12.60%**	**6.80%**	**6.29**	**7.65**
550	0.80	0.83	11.00%	10.00%	7.25	8.25
750	1.15	1.12	15.00%	12.00%	7.65	9.30
2000	1.28	0.41	14.00%	6.00%	9.18	6.91
4000	0.45	0.17	12.00%	3.00%	3.72	5.66
10000	0.29	0.07	11.00%	3.00%	2.62	2.49
U	**0.58**	**0.35**	**12.00%**	**6.40%**	**4.86**	**5.44**
550	0.44	0.63	8.00%	9.00%	5.52	7.03
750	0.80	0.92	15.00%	12.00%	5.31	7.64
2000	1.28	0.19	16.00%	6.00%	8.00	3.10
4000	0.14	0.00	11.00%	3.00%	1.28	0.14
10000	0.26	0.00	10.00%	2.00%	2.55	0.04
O	**0.18**	**0.10**	**6.80%**	**2.60%**	**2.69**	**3.84**
550	0.10	0.11	3.00%	3.00%	3.24	3.71
750	0.24	0.27	7.00%	4.00%	3.48	6.76
2000	0.40	0.12	9.00%	4.00%	4.50	2.92
4000	0.15	0.00	7.00%	1.00%	2.11	0.01
10000	0.02	0.00	8.00%	1.00%	0.26	0.00
S4-DBR	**0.89**	**0.68**	**12.45%**	**7.75%**	**7.18**	**8.79**

Information Only

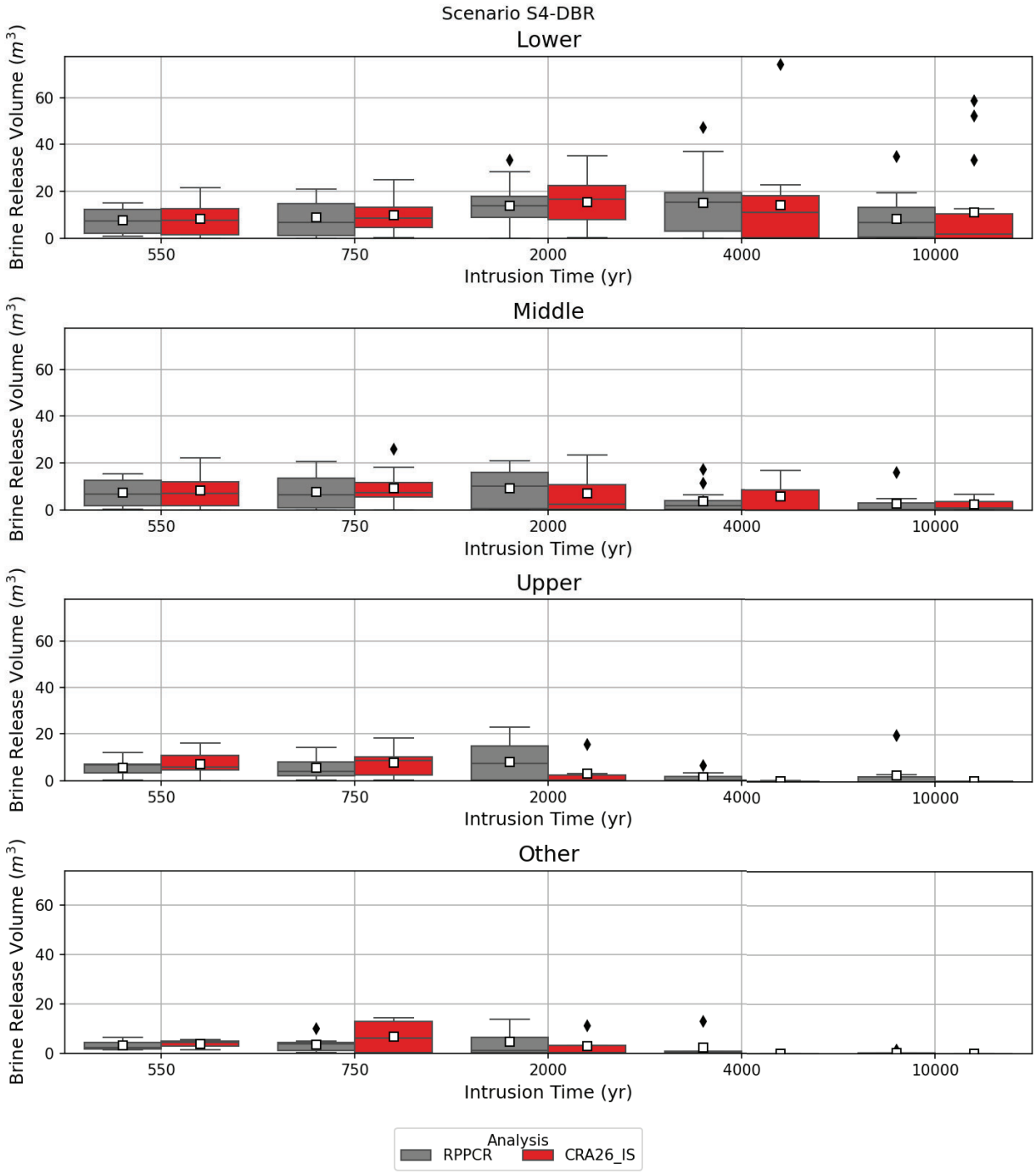

Figure 12. S4-DBR Volumes, All Non-Zero Releases, Replicate 1

Information Only

5.5 Maximum Releases

The ten largest brine release volumes for the CRA26_IS and RPPCR are shown in Table 8. The ten largest DBR volumes increased significantly in the CRA26_IS compared to the RPPCR. Note that the absolute largest release volumes for each analysis do not necessarily come from simulations with the highest saturation or pressure. From the table:

(i) For the CRA26_IS, the ten largest DBR volumes exceed all ten from the RPPCR and the mean of the ten largest volumes increased by about 40%.

(ii) All of the largest CRA26_IS DBR volumes came from the L intrusion location. All but one of the RPPCR largest volumes came from the L intrusion.

(iii) The mean brine pressure of the largest ten DBR volumes increased by about 1.5% between the two analyses, while the mean brine saturation decreased by about 10%. Thus the impact to DBR volumes due to the relatively small increase in brine pressures exceeded the impact due to the larger decrease in brine saturation. The impact of the lower saturations is minimal as long as the saturation exceeds the minimum saturation required for a DBR.

(iv) For the CRA26_IS, five of the largest volumes came from scenarios with a previous E2 intrusion; three came from scenarios with a previous E1 intrusion; and two were from scenarios with no previous intrusion. For the RPPCR, four of the largest volumes came from scenarios with a previous E2 intrusion; three came from scenarios with a previous E1 intrusion; and three were from scenarios with no previous intrusion.

(v) For the CRA26_IS, one vector (Replicate 1, Vector 28) was associated with five top releases. For the RPPCR, the same vector was associated with the three top releases, and five out of the top ten.

Information Only

Table 8. Largest DBR Volumes by Analysis

Analysis	Rank	Replicate	Scenario	Time (yr)	Vector	Location	Release (m^3)	Pressure (MPa)	Saturation (-)
RPPCR	1	1	4	4000	28	L	47.383	15.350	0.948
RPPCR	2	1	2	4000	28	L	47.254	15.343	0.948
RPPCR	3	1	5	3000	28	L	45.737	15.487	0.948
RPPCR	4	1	1	10000	8	L	42.107	15.382	0.864
RPPCR	5	1	5	5000	28	L	40.944	14.563	0.948
RPPCR	6	1	2	10000	6	L	40.446	15.304	0.990
RPPCR	7	1	5	5000	28	M	38.854	14.516	0.819
RPPCR	8	3	2	10000	15	L	38.125	15.316	0.996
RPPCR	9	2	1	10000	63	L	37.921	15.271	0.937
RPPCR	10	2	1	5000	78	L	37.207	15.327	0.991
						Mean	**41.598**	**15.186**	**0.939**
CRA26_IS	1	1	4	4000	28	L	74.023	15.827	0.742
CRA26_IS	2	1	3	5000	28	L	69.393	15.586	0.763
CRA26_IS	3	1	5	10000	28	L	58.898	15.159	0.948
CRA26_IS	4	1	4	10000	28	L	58.624	15.157	0.948
CRA26_IS	5	1	2	10000	28	L	58.441	15.153	0.948
CRA26_IS	6	1	2	10000	6	L	53.317	15.372	0.773
CRA26_IS	7	1	5	10000	5	L	52.840	15.425	0.838
CRA26_IS	8	2	1	10000	63	L	52.437	15.393	0.783
CRA26_IS	9	1	4	10000	5	L	52.054	15.422	0.841
CRA26_IS	10	2	1	5000	63	L	47.859	15.705	0.936
						Mean	**57.789**	**15.420**	**0.852**

Information Only

6.0 DRIVERS AND CORRELATIONS

Volume-averaged brine pressure and brine saturation in the intruded panel are the two most important variables that control DBR volumes (Clayton et al. 2008). In this section, brine pressure and saturation initial conditions for the DBR simulations are summarized and compared for the CRA26_IS and RPPCR analyses. For a discussion of the modeling setup that produces the initial conditions, and a more comprehensive analysis of those results, see the CRA26_IS Salado flow analysis report (Day and King 2025).

As has been done for previous DBR analysis reports (e.g., Docherty and King 2023), sensitivity of DBR volumes to brine pressure and saturation initial conditions will also be qualitatively examined. Pressure and saturation values were extracted from the ALGEBRACDB output files generated as a preprocessing step for the DBR input (Figure 5). Pressure and saturation values were extracted from the intruded regions, and so represent the pressure and saturation conditions encountered by the intrusions.

In previous reports (e.g., Stoelzel and O'Brien 1996 and Docherty and King 2023), only scenario S2-DBR was discussed in the presentation of initial conditions and the sensitivity analysis. Scenario S2-DBR has the greatest number of non-zero releases in both the RPPCR and the CRA26_IS (Figure 9). However, the observed differences between the RPPCR and the CRA26_IS for the S4-DBR scenario has led to a discussion of its initial conditions in this report (see Section 6.1.2). For the two analyses, all four intrusion locations are examined for comparison.

The sensitivity of DBR volumes to those parameters that most influence brine pressure and saturation in the CRA26_IS Salado flow simulations is illustrated in Appendix A.

6.1 Initial Conditions Summary

Initial conditions for DBR volume calculations come from Salado flow model results. The initial conditions of brine pressure and brine saturation at the time of intrusion are discussed in this section for scenarios S2-DBR and S4-DBR.

6.1.1 S2-DBR

CRA26_IS DBR mean initial conditions are presented for the S2-DBR scenario in Table 9 with RPPCR values for comparison. Boxplots of initial pressure and saturation are shown in Figure 13 and Figure 14. Mean initial brine pressures for L, M and U intrusion locations are increased, but similar, in the CRA26_IS compared to the RPPCR; the increases are seen at all intrusion times. Median initial brine pressures for these intrusion locations are also generally slightly increased or similar, with the exception of the year 4,000 intrusion for the L and M locations (Figure 13). Maximum initial brine pressures are slightly greater in the CRA26_IS at each intrusion time; the maximum pressures increase with time except for the year 10,000 intrusion. In the case of the O intrusion location, mean pressures are slightly decreased and median pressures are slightly decreased or similar. Note also that mean initial brine pressures for the L and M locations reach a maximum for the year 2,000 intrusion, while for the U and O locations, they increase with intrusion

Information Only

time in both the CRA26_IS and the RPPCR (with the one exception of a slight decrease for the RPPCR year 10,000 intrusion), consistent with the results of Day and King (2025).

For the L and M locations, most intrusions encounter pressure conditions above the 8 MPa threshold for a DBR – this is true for both the CRA26_IS and the RPPCR. For the U location, approximately the same number of intrusions encounter the 8 MPa threshold in the CRA26_IS and the RPPCR; most intrusions at the year 750 intrusion time and earlier do not encounter the 8 MPa threshold and most of the intrusions at the year 2,000 intrusion time and later do encounter the 8 MPa threshold. Mean pressures at the O location in both analyses exceed the 8 MPa threshold only at the year 10,000 intrusion time.

Mean and median brine saturations in the CRA26_IS decreased at all locations compared to the RPPCR (Figure 14). Intrusions at the L and M locations encountered approximately the entire range of saturations (0 to 1) across all times, although the distribution of saturations is shifted lower for the CRA26_IS. Intrusions at the U and O locations encountered a slightly reduced upper range of saturations, with maximum saturation decreasing from the RPPCR to the CRA26_IS at the year 2,000 intrusion time and later for the U location and at all times for the O location. For both analyses, mean saturation tends to decrease with time, reaching a minimum at the year 4,000 or 10,000 year intrusion at all locations.

Information Only

Table 9. S2-DBR Mean Initial Conditions, Replicate 1

Intrusion Location and Time (yr)	Brine Pressure (MPa)		Brine Saturation (-)	
	RPPCR	CRA26_IS	RPPCR	CRA26_IS
L	**11.36**	**11.68**	**0.65**	**0.46**
550	10.02	10.44	0.78	0.64
750	11.43	11.87	0.76	0.62
2000	12.54	12.58	0.65	0.46
4000	11.98	12.10	0.52	0.29
10000	10.83	11.38	0.53	0.28
M	**11.34**	**11.66**	**0.40**	**0.26**
550	9.99	10.42	0.61	0.49
750	11.40	11.86	0.57	0.43
2000	12.52	12.57	0.40	0.21
4000	11.97	12.10	0.24	0.10
10000	10.82	11.37	0.18	0.07
U	**8.50**	**8.78**	**0.13**	**0.07**
550	4.97	5.19	0.19	0.13
750	6.42	6.80	0.18	0.12
2000	9.86	10.07	0.13	0.05
4000	10.74	10.91	0.08	0.03
10000	10.51	10.93	0.07	0.03
O	**5.42**	**5.19**	**0.10**	**0.05**
550	3.01	2.81	0.16	0.10
750	3.49	3.24	0.15	0.08
2000	5.21	5.00	0.10	0.04
4000	6.83	6.51	0.06	0.02
10000	8.58	8.39	0.06	0.03
S2-DBR	**9.16**	**9.33**	**0.32**	**0.21**

Information Only

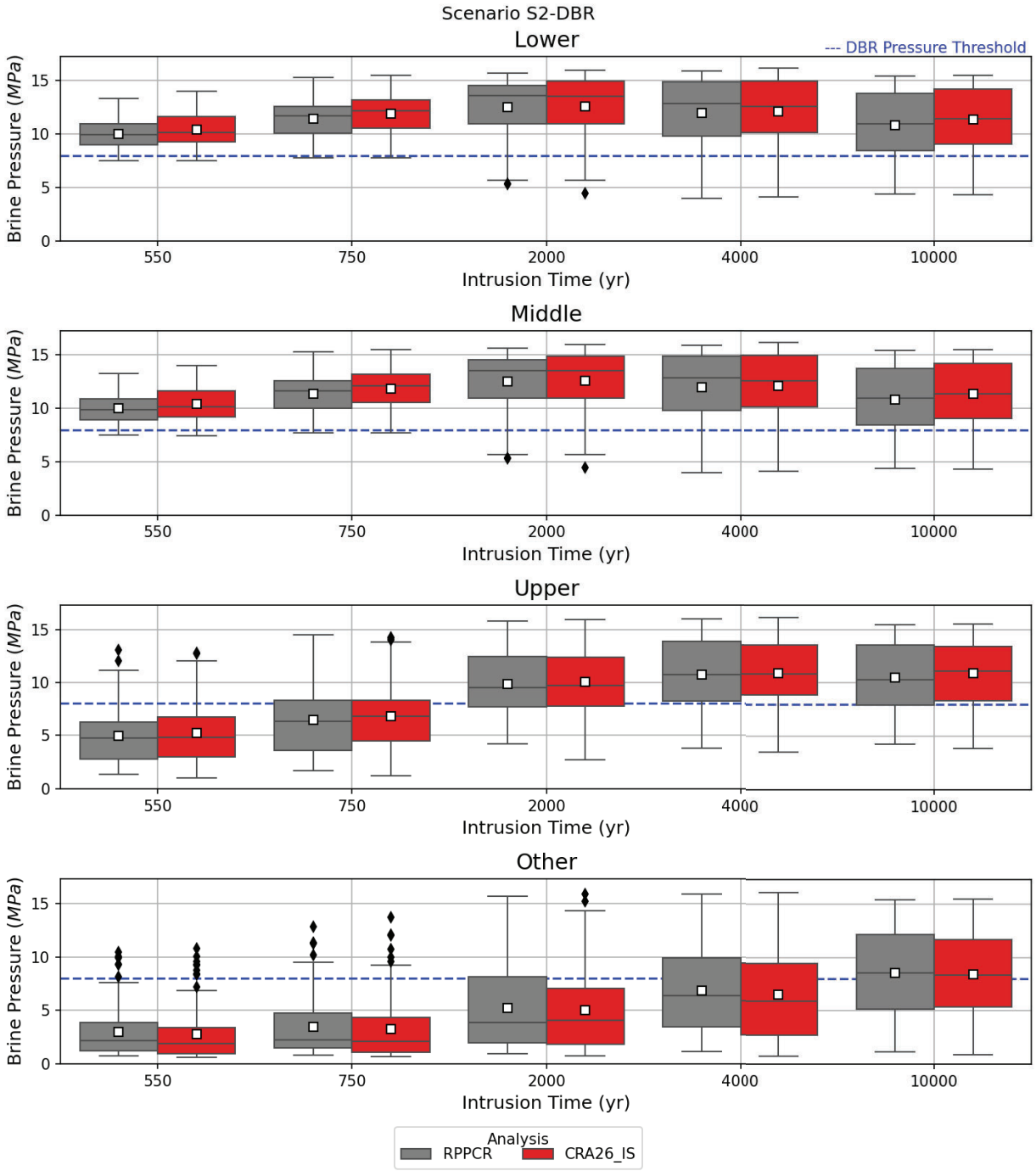

Figure 13. S2-DBR Brine Pressure, All Intrusions, Replicate 1

Information Only

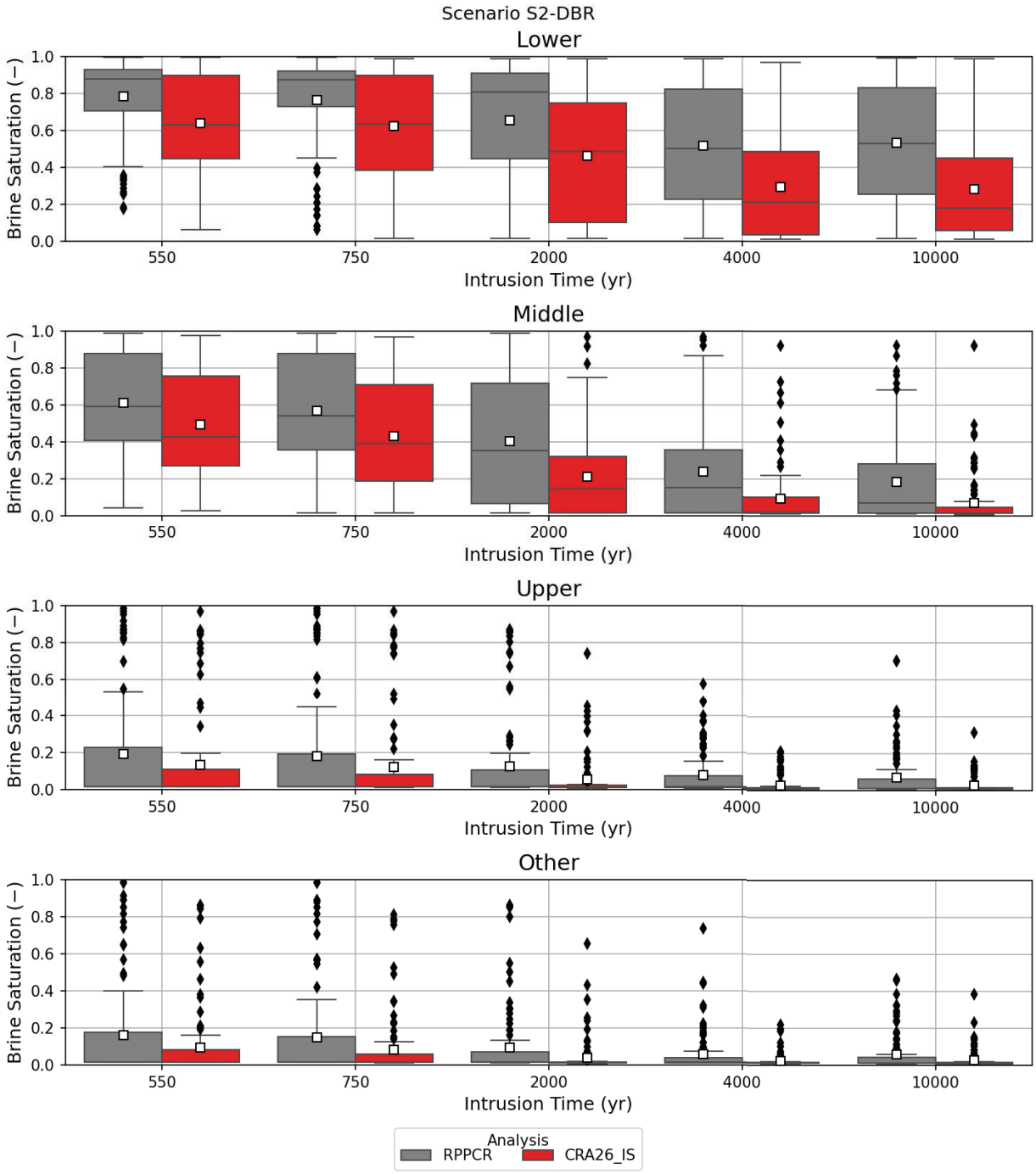

Figure 14. S2-DBR Brine Saturation, All Intrusions, Replicate 1

Information Only

6.1.2 S4-DBR

For the S4-DBR scenario, mean initial conditions are presented in Table 10, with boxplots shown in Figure 15 and Figure 16. Mean and median initial brine pressures for all intrusion locations are decreased (in contrast to the S2-DBR scenario) in the CRA26_IS compared to the RPPCR; the decreases are seen at all intrusion times (Table 10 and Figure 15). However, maximum initial brine pressures are similar or only slightly greater in the CRA26_IS. Note also that initial brine pressures tend to increase with intrusion time for all intrusion locations in both the CRA26_IS and the RPPCR, as expected from the results of Day and King (2025).

For all locations, most intrusions encounter pressure conditions below the 8 MPa threshold for a DBR – this is true for both the CRA26_IS and the RPPCR. This is in contrast to the S2-DBR scenario, but expected due to the lack of previous intersection with pressurized brine in the Castile.

Mean and median brine saturations in the CRA26_IS decreased at all locations compared to the RPPCR (Figure 16). Intrusions at the L and M locations encountered approximately the same range (i.e., minimum and maximum) of saturations between analyses across all times. Intrusions at the U and O locations encountered a slightly reduced upper range of saturations, with maximum saturation decreasing for the CRA26_IS at the year 750 intrusion time and later for the U location and at all times for the O location. For both analyses, saturation tends to decrease, with time at all locations, reaching a minimum at the year 4,000 or 10,000 year intrusion. The saturation trends are similar to those for the S2-DBR scenario.

Information Only

Table 10. S4-DBR Mean Initial Conditions, Replicate 1

Intrusion Location and Time (yr)	Brine Pressure (MPa)		Brine Saturation (-)	
	RPPCR	CRA26_IS	RPPCR	CRA26_IS
L	**6.15**	**5.65**	**0.29**	**0.20**
550	4.21	4.06	0.32	0.25
750	4.86	4.60	0.31	0.24
2000	6.54	5.95	0.27	0.18
4000	7.35	6.53	0.25	0.15
10000	7.79	7.11	0.28	0.17
M	**6.14**	**5.65**	**0.13**	**0.08**
550	4.20	4.05	0.20	0.13
750	4.85	4.60	0.18	0.12
2000	6.53	5.95	0.13	0.06
4000	7.35	6.53	0.09	0.03
10000	7.78	7.11	0.08	0.04
U	**5.92**	**5.37**	**0.13**	**0.07**
550	3.83	3.71	0.19	0.13
750	4.54	4.31	0.18	0.12
2000	6.28	5.68	0.13	0.05
4000	7.17	6.25	0.07	0.03
10000	7.77	6.91	0.07	0.03
O	**4.70**	**3.90**	**0.10**	**0.05**
550	2.99	2.78	0.16	0.10
750	3.42	3.09	0.15	0.08
2000	4.61	3.86	0.10	0.04
4000	5.60	4.36	0.06	0.02
10000	6.89	5.42	0.06	0.03
S4-DBR	**5.73**	**5.14**	**0.16**	**0.10**

Information Only

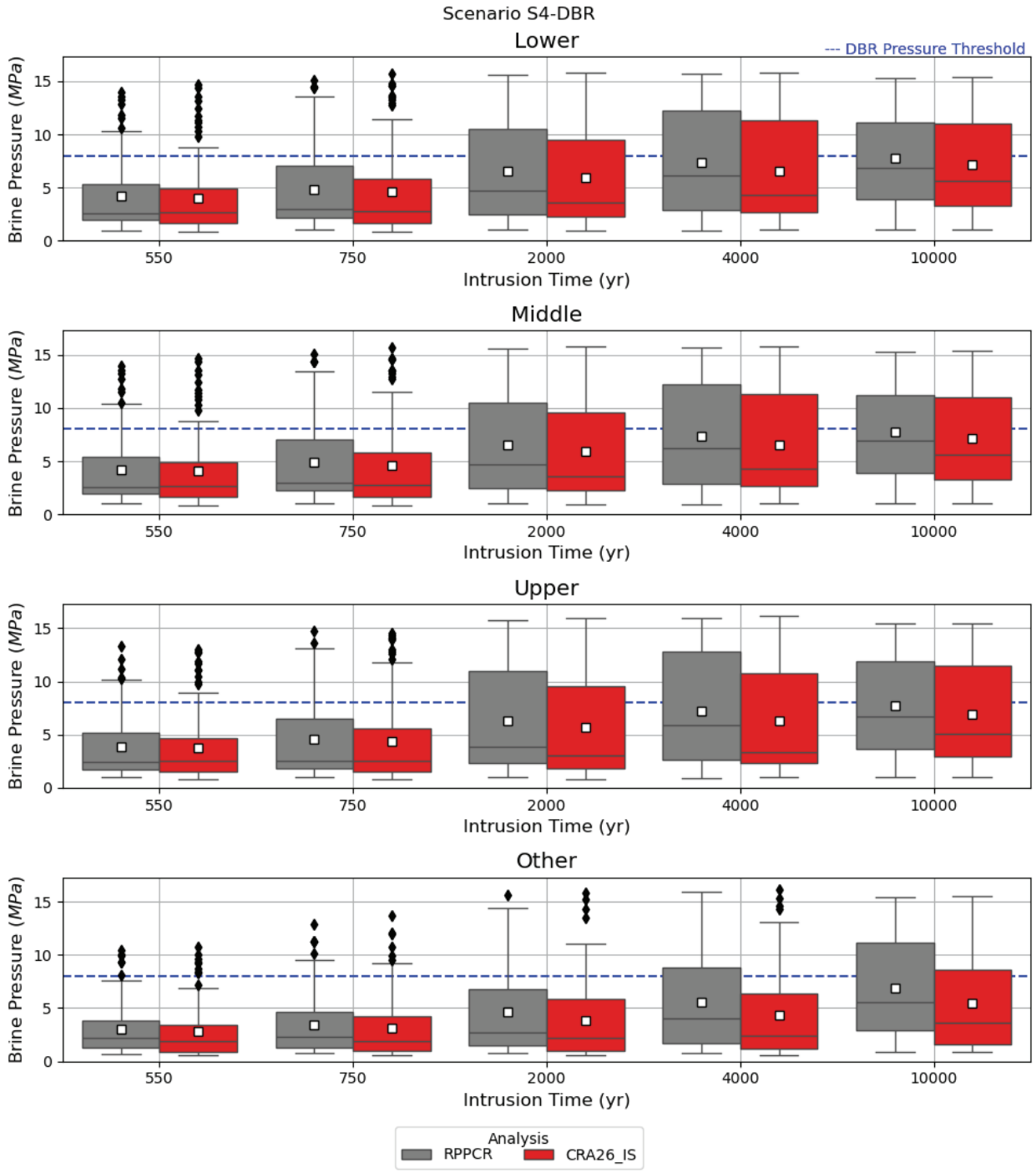

Figure 15. S4-DBR Brine Pressure, All Intrusions, Replicate 1

Information Only

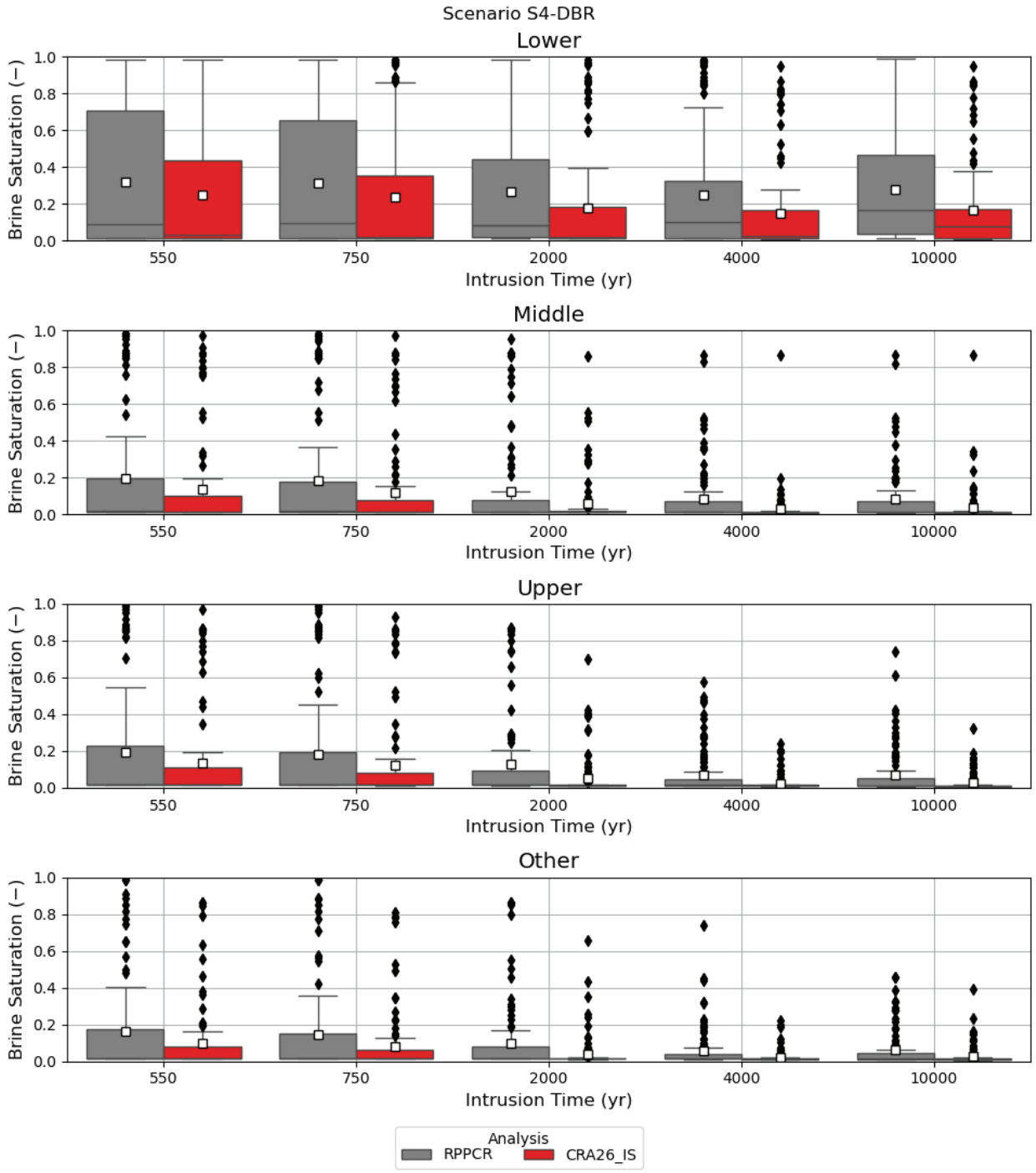

Figure 16. S4-DBR Brine Saturation, All Intrusions, Replicate 1

Information Only

6.2 Correlation and Sensitivity to Initial Conditions

Scatter plots were created to visualize the correlation and sensitivity of CRA26_IS DBR volume to initial panel pressure and saturation (Figure 17 and Figure 18, respectively) with the RPPCR plotted separately for comparison. As was done in previous DBR analysis reports, saturation is plotted as mobile brine saturation, calculated as brine saturation less the residual brine saturation (Stoelzel and O'Brien 1996 and Docherty and King 2023). Regression statistics were calculated with the python SciPy[1] statistics package, and the line of best fit plotted over the data. Simulations with zero releases were not plotted or included in the regression analysis.

Each simulation was categorized into flow regimes from the ratio of relative permeabilities of brine and gas, as is done in the ALGEBRACDB preprocessing step to calculate flowing bottom hole pressure (Equation 1 and Stoelzel and O'Brien 1996). Simulations were categorized as "all brine" if the gas relative permeability is zero (equivalently, the gas saturation is the residual gas saturation), "brine dominated" if the gas relative permeability is lower than the brine relative permeability, and "gas dominated" if the gas relative permeability is higher than the brine relative permeability. There were no observations in "all brine" category for either analysis (i.e., gas relative permeability never reaches zero), but this was observed for the CRA-2019 PA (Docherty and King 2023). Because flow regime is a function of both brine saturations and residual brine saturation, the same brine saturation can be categorized into multiple flow regimes (Figure 19 and Figure 20).

For the CRA26_IS, Figure 17 (bottom) shows brine pressure has the strongest correlation with brine release volume when the panel is under a brine dominated flow regime. (Here, strength of correlation is measured by the coefficient of correlation, reported as "r^2" in the figure.) When the flow regime is gas dominated, brine pressure has little correlation with release volume.

Figure 17 (top) shows brine dominated and gas dominated flow regimes for the RPPCR. Similar to the CRA26_IS, initial brine pressure has the strongest correlation with brine release volume in the brine dominated regime and when the RPPCR flow regime is gas dominated there is little correlation with release volume. Note also that DBR volumes are slightly more, but similarly, sensitive to pressure in the CRA26_IS: the slope of the straight line fit in the CRA26_IS brine dominated flow regime is slightly greater than the brine dominated line slope in the RPPCR.

Figure 18 shows brine saturation has the strongest correlation with brine release volumes under gas dominated flow regimes. There does not appear to be any relationship between brine release and saturation under brine dominated flow regimes in the RPPCR or the CRA26_IS. For the gas dominated flows, the sensitivity of DBR volume to mobile brine saturation in the RPPCR is about 1.5 times the CRA26_IS sensitivity, with about the same correlation.

Taken together, these results indicate: (i) if brine saturation is low so that the flow is gas dominated, then DBR intrusions are more sensitive to panel saturation than they are to panel pressure; and (ii) if brine saturation increases enough to produce a brine dominated flow regime, then panel brine saturation becomes less important and DBR volumes are more sensitive to panel brine pressure.

[1] SciPy is a Python-based ecosystem of open-source software for mathematics, science, and engineering. https://www.scipy.org

Information Only

Figure 19 shows the frequency of non-zero DBR volumes versus mobile brine saturation for the S2-DBR scenario at the L and M intrusion locations. In Section 5.3 it was noted that the frequency of non-zero DBR volumes at these locations decreased from the RPPCR to the CRA26_IS, and that the mean non-zero release volumes in the CRA26_IS is about one 20-30% less than the means in the RPPCR. Figure 19 indicates more DBR volumes are occurring at lower panel saturations in the CRA26_IS at the L and M locations. Figure 20 shows the DBR volume frequencies at the U and O intrusion locations. Compared to the RPPCR, frequencies have decreased for all saturations at the U and O intrusion locations; however, the numbers are small.

Information Only

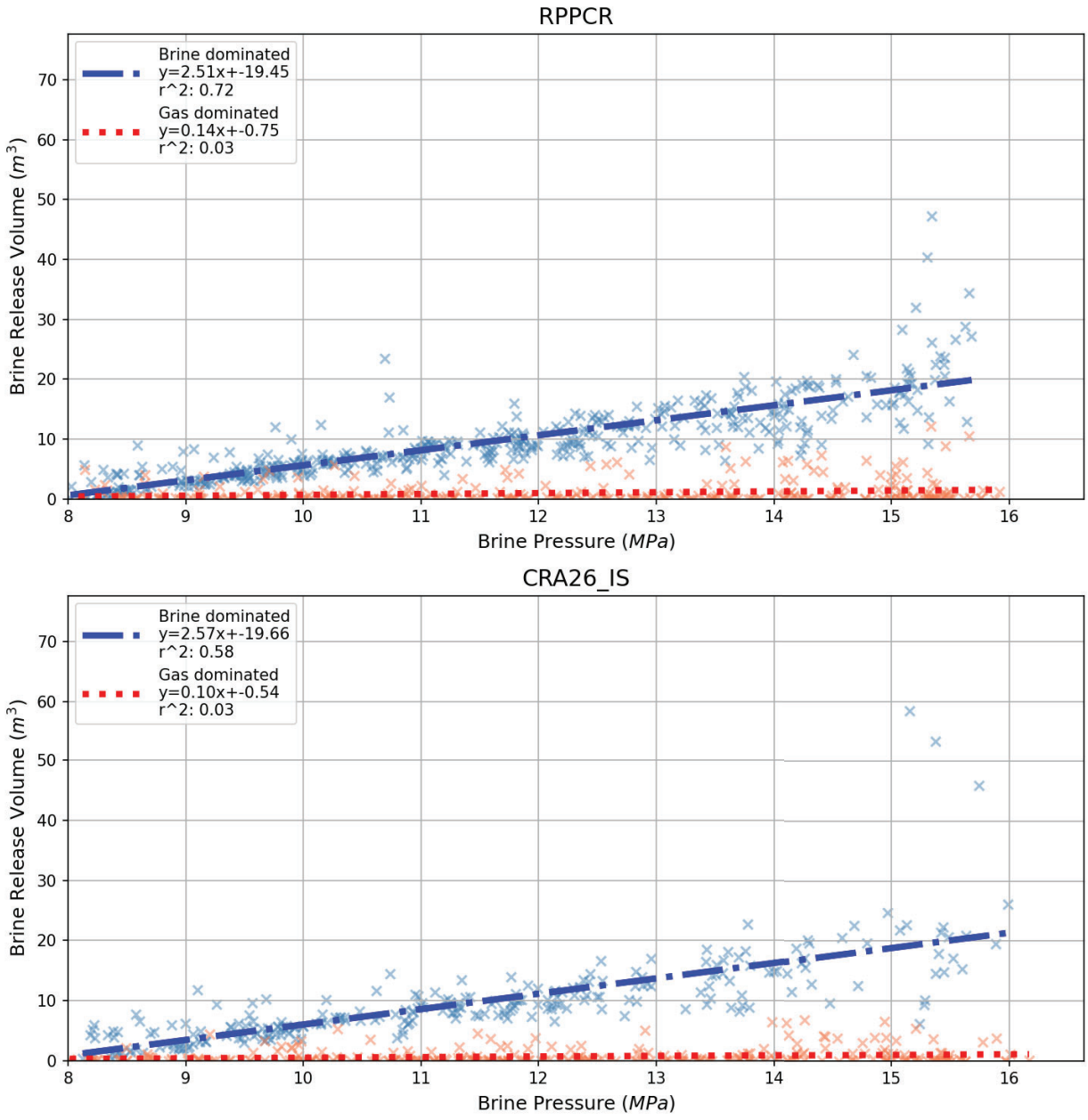

Figure 17. S2-DBR Release Volume Versus Brine Pressure, All Non-Zero Intrusions, Replicate 1

Information Only

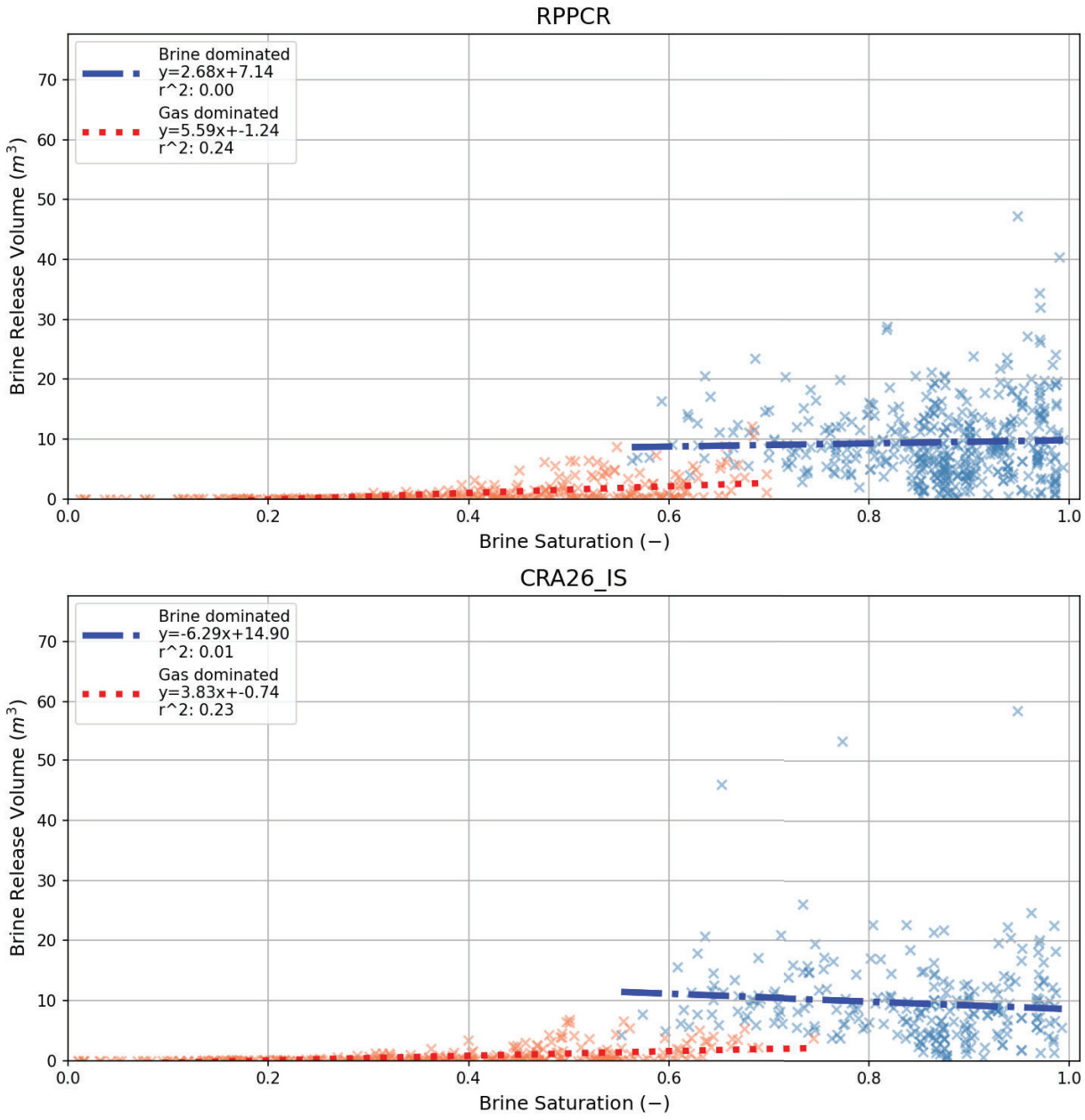

Figure 18. S2-DBR Release Volume Versus Brine Saturation, All Non-Zero Intrusions, Replicate 1

Information Only

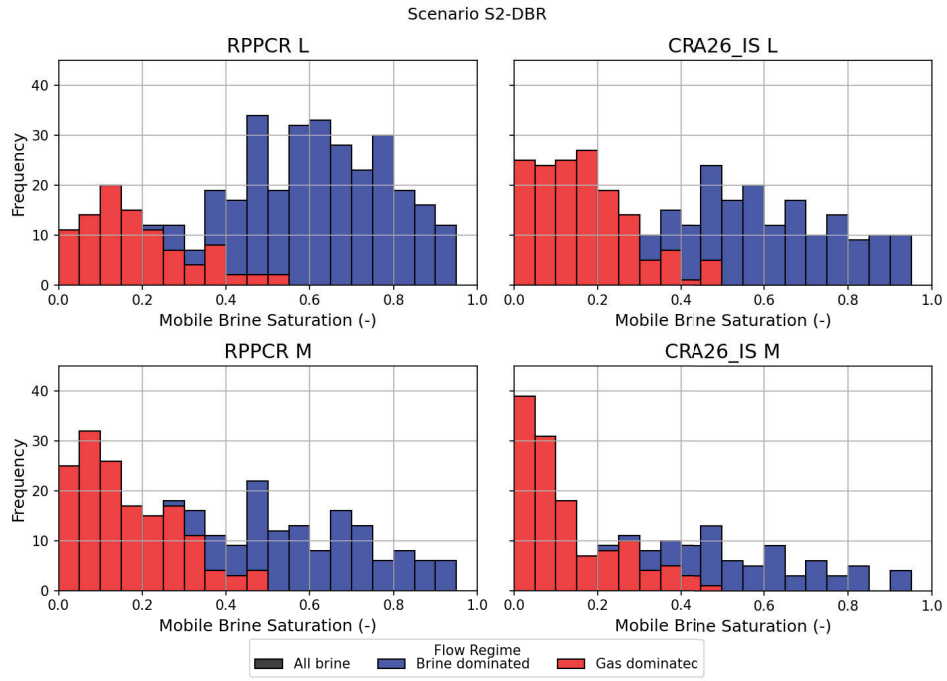

Figure 19. Brine Saturation Frequency, S2-DBR All Lower and Middle Intrusions, Replicate 1

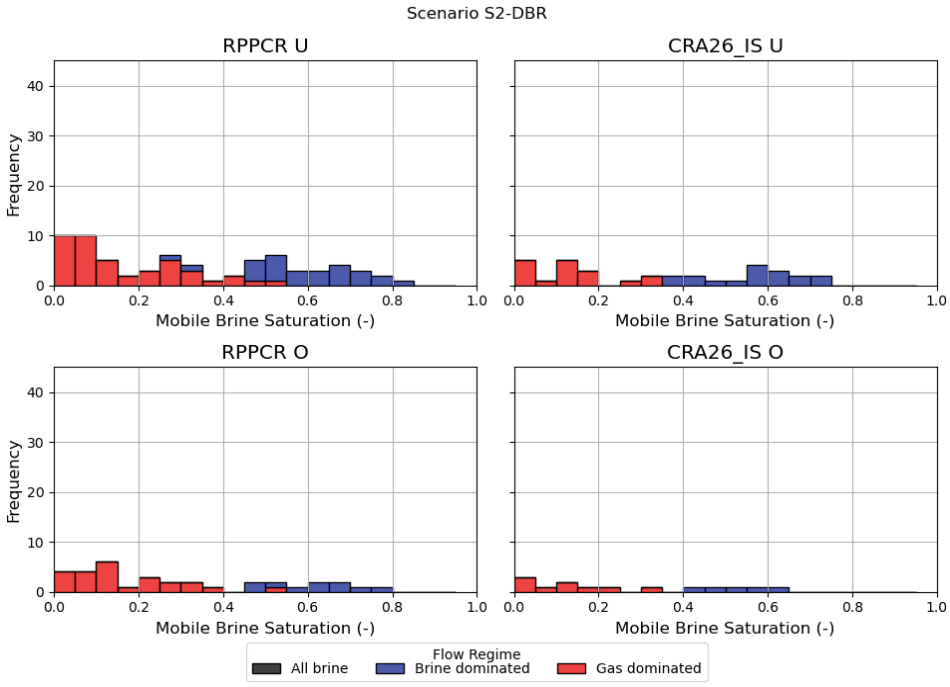

Figure 20. Brine Saturation Frequency, S2-DBR All Upper and Other Intrusions, Replicate 1

Information Only

7.0 SUMMARY

Due to their importance with respect to DBR probabilities calculated using the CCDFGF code, the predicted DBR volumes for four intrusion locations over the representative scenarios are summarized for the CRA26_IS in comparison to the RPPCR. There were no direct changes to model input parameters between the RPPCR and CRA26_IS. However, there were several changes to Salado flow inputs that impact DBR results via the initial conditions to a DBR, that is the brine saturations and brine pressures. The reduced number of waste panels represented in the CRA26_IS Salado flow calculations did not result in a change to the DBR grid implemented for CRA26_IS, as it already adequately considers the connections between the Salado flow results and DBR initial conditions for each of the waste regions. With the short duration of DBR simulations, there is very little communication across panel closures; therefore, there is not a need to have an explicit representation of repository volume outside of the panel closures containing the intrusion locations.

A comparison of results between the RPPCR and CRA26_IS was made primarily for Replicate 1, but some differences among the replicates are discussed. Compared to the RPPCR, the number of non-zero DBR volumes decreased in the CRA26_IS across all scenarios. The number of small magnitude releases decreased and the number of large magnitude releases increased slightly in the CRA26_IS (in two of the three replicates).

The overall mean non-zero release volume in the CRA26_IS decreased by about 10% from the mean non-zero release volume in the RPPCR. For the CRA26_IS, mean non-zero release volumes decreased for scenarios S1-DBR, S2-DBR, and S3-DBR, but increased for the other two scenarios. Median release volumes are decreased for all scenarios except S4-DBR. Maximum release volumes are increased for all scenarios except S1-DBR.

In both the CRA26_IS and the RPPCR, the largest DBR volumes occurred at the L borehole intrusion location, situated in the down-dip Lower waste region. DBR volumes from the O borehole location in both analyses made up only a small fraction of the DBR volumes from all intrusion locations.

The RPPCR Salado flow model (Day and King 2025) showed a decrease in mean brine pressures for scenarios without an E1 intrusion and an increase in mean brine pressures for scenarios with an E1 intrusion (except for the westernmost waste areas). Additionally, there is an observed decrease in brine saturation. The combination of these effects could lead to mixed impacts on the number of non-zero DBR volumes across scenarios. Day and King (2025) also points out that maximum brine pressure for any individual vector in Replicate 1 is generally greater in the CRA26_IS and there is a substantial decrease in brine saturation; these are effects that could also lead to mixed impacts on the magnitudes of the largest DBR volumes. The decrease in mean non-zero release volumes can be attributed to reduced brine saturation for scenarios with E1 intrusion, despite increased brine pressures (Day and King 2025) and the observed increase in the number of large magnitude releases. The increased mean DBR volumes for scenarios S4-DBR and S5-DBR can be attributed to increased maximum pressures in CRA26_IS.

In the Salado flow model, the decreased waste area footprint and waste area volume in the West Rest-of-Repository compared to the RPPCR led to reduced brine inflow and increased relative

Information Only

brine consumption. These result in reduced pressures in non-Castile intruded scenarios which are used as initial brine pressures in DBR volume calculations. Increased gas generation and similar brine saturations following intrusions in the Salado flow model for CRA26_IS are also noted and explain increased pressures in comparison to RPPCR for scenarios with Castile intrusions. Overall, a substantial decrease in brine saturation in all waste areas over all Salado flow scenarios was observed, leading to reduced brine saturation initial conditions for DBR volume calculations. Although the focus of the report is on the results from Replicate 1, and there are some observed differences among the replicates, the Replicate 1 results are generally representative of the overall DBR volume results.

Information Only

8.0 REFERENCES

Bollinger, M. 2024. Letter to Ms. L. Veal. Subject: Planned Change Request for the use of Replacement Panels 11 and 12. March 12, 2024. CBFO:ERCD:MG:SV:24-0168. Carlsbad, NM: U.S. DOE, Carlsbad Field Office.

Brooks, R.H. and A.T. Corey. 1964. Hydraulic properties of porous media, Hydrology Paper no. 3. Fort Collins, CO: Civil Engineering Department, Colorado State University.

Brunell, S. 2025. Update to CRA-2026 PA Input Parameters Due to Revised WIPP Repository Dimensions. EIMS-0004799007. Carlsbad, NM: Sandia National Laboratories.

Chappelear, J.E., and A.S. Williamson. 1981. Representing Wells in Numerical Reservoir Simulation: Part 2—Implementation. Society of Petroleum Engineers Journal, vol. 21: 339–44.

Clayton, D.J., S. Dunagan, J.W. Garner, A.E. Ismail, T.B. Kirchner, G.R. Kirkes, M.B. Nemer. 2008. Summary Report of the 2009 Compliance Recertification Application Performance Assessment. ERMS 548862. Carlsbad, NM: Sandia National Laboratories.

Day, B. and S. King. 2025. Analysis Report for Salado Flow in the 2026 Compliance Recertification Application Performance Assessment: Interim State Repository. EIMS-0004944216. Carlsbad, NM: Sandia National Laboratories.

Day, B. 2025a. BRAGFLO Grid Development for CRA-2026. EIMS-0004447000. Carlsbad, NM: Sandia National Laboratories.

Day, B. 2025b. Recommendation and Justification for Implementing a Lower Bound on Capillary Pressure in Marker Bed Materials S_MB139, S_ANH_AB, and S_MB138 using the CAP_MOD and PO_MIN Parameters for CRA-2026. EIMS-0004430534. Carlsbad, NM: Sandia National Laboratories.

Docherty, P. and S. King. 2023. Direct Brine Release Analysis Report for the Replacement Panels Planned Change Request (RPPCR). ERMS 579724. Carlsbad, NM: Sandia National Laboratories.

Domski, P. 2025a. Parameter Memorandum: Uncertainty Analysis of Actinide Solubilities for the 2026 Compliance Recertification Application (CRA-2026). EIMS-0004447122. Carlsbad, NM: Sandia National Laboratories.

Domski, P. 2025b. Th(IV), Np(V), and Am(III) Baseline Solubilities for the 2026 WIPP Compliance Recertification Application Performance Assessment Interim-State Analysis (CRA-2026 IS). EIMS-0004833660. Carlsbad, NM: Sandia National Laboratories.

Hansen, C., S. Brunell, B. Day, S. King, and J. Wilgus. 2025. Analysis Plan for the 2026 WIPP Compliance Recertification Application Performance Assessment. AP-214. Carlsbad, NM: Sandia National Laboratories.

Helton, J.C., J.E. Bean, J.W. Berglund, F.J. Davis, K. Economy, J.W. Garner, J.D. Johnson, R.J., MacKinnon, J. Miller, D.G. O'Brien, J.L. Ramsey, J.D. Schreiber, A. Shinta, L.N. Smith, D.M. Stoelzel, C. Stockman, and P. Vaughn. 1998. Uncertainty and Sensitivity Analysis Results

Information Only

Obtained in the 1996 Performance Assessment for the Waste Isolation Pilot Plant. SAND98-0365. ERMS 252619. Albuquerque, NM: Sandia National Laboratories.

Kaplan, U., Swanson, J., and Kutahyali-Aslani, C. 2025. LANL ACRSP Parameter Recommendations for CRA-2026 Performance Assessment. Revision 1. LCO-ACP-41. Carlsbad, NM: Los Alamos National Laboratory.

Kicker, D. 2025. Analysis Report for Radionuclide Inventory Screening in the 2026 Compliance Recertification Application Performance Assessment: Interim State Repository. Revision 0. EIMS-0004832100. Carlsbad, NM: Sandia National Laboratories.

King, S. 2023. Salado Flow Analysis Report for the Replacement Panels Planned Change Request (RPPCR). ERMS 579722. Carlsbad, NM: Sandia National Laboratories.

King, S. 2025a. Constructed Cumulative Distributions for Approximation of Truncated Normal Distributions. EIMS-0004799476. Carlsbad, NM: Sandia National Laboratories.

King, S. 2025b. Area for RH waste disposal for the interim state CRA-2026 PA calculation. EIMS-0004801801. Carlsbad, NM: Sandia National Laboratories.

Kirkes, R. 2007. Evaluation of the Duration of Direct Brine Release in WIPP Performance Assessment (Revision 0). ERMS 545988. Carlsbad, NM: Sandia National Laboratories.

Knerr, R. 2020. Letter to Ms. Lee Ann B. Veal, U.S. Environmental Protection Agency, subject: "Planned Change Request for Alternative Panel Closure Locations for Panels 1 and 2," Carlsbad, NM: U.S. DOE, Carlsbad Field Office.

Long, J. 2025. Computational Code Execution and File Management in the 2026 Compliance Recertification Application Performance Assessment: Interim State Repository. EIMS-0004900878. Carlsbad, NM: Sandia National Laboratories.

Mariner P. 2025. CRA-2026 IS updates to the WIPP humic colloids models for An(III) and An(IV). EIMS-0004838142. Carlsbad, NM: Sandia National Laboratories.

Mattax, C.C. and R.L. Dalton. 1990. Reservoir Simulation. Richardson, TX: Henry L. Doherty Memorial Fund of AIME, Society of Petroleum Engineers.

Nemer, M. 2025. MgO Hydration Rates for the CRA-2026 Under AP-208. EIMS-0004445255. Albuquerque, NM: Sandia National Laboratories.

Stoelzel, D.M., and D.G. O'Brien. 1996. Analysis Package for the BRAGFLO Direct Release Calculations (Task 4) of the Performance Assessment Calculations Supporting the Compliance Certification Application (CCA), AP-029, Brine Release Calculations. ERMS 417870. Albuquerque, NM: Sandia National Laboratories.

U.S. Environmental Protection Agency (U.S. EPA). 1998. 40 CFR Part 194: Criteria for the Certification and Recertification of the Waste Isolation Pilot Plant's Compliance with the Disposal Regulations: Certification Decision. Federal Register, vol. 63 (May 18, 1998): 27354 – 27406.

U.S. Environmental Protection Agency (U.S. EPA). 2025. Letter from Abigale Tardif to Mark Bollinger, Subject: EPA's Review and Approval of DOE's RPPCR for Waste Panels 11 and 12 at WIPP. July 31, 2025. Washington, DC: U.S. EPA.

Information Only

Van Soest, G. 2025. Interim State Performance Assessment Inventory Report – 2024. Revision 0. INV-IPA-24. Carlsbad, NM: Los Alamos National Laboratory.

Ward, A. 2025. Performance Assessment Inventory for Analysis of a 12-Panel Repository Configuration. Letter to Bill McInroy. March 18, 2025. CBFO:ERCD:AW:RS:25-0197. Carlsbad, NM: Department of Energy Carlsbad Field Office.

WIPP PA. 2025. Design Document and User's Manual for BRAGFLO Version 8.00. EIMS-0004430695. Carlsbad, NM: Sandia National Laboratories.

Information Only

9.0 APPENDIX A – SENSITIVITY TO INPUT PARAMETERS

Brine pressure and saturation are the two most important drivers of DBR volumes, consequently the sampled parameters that control variability in brine pressure and saturation also control variability in DBR volumes. Since scenarios with a previous E1 intrusion drive non-zero DBR volumes, dominant parameters affecting waste panel pressure and saturation for the Salado flow S2-BF scenario are discussed in this Appendix. The dominant parameters were determined using a STEPWISE analysis (Day and King 2025).

For waste panel pressure in the CRA26_IS S2-BF scenario, the intact halite porosity parameter S_HALITE:POROSITY is dominant, followed by the long-term borehole permeability BH_SAND:PRMX_LOG, and the probability of plastic and rubber biodegradation parameter WAS_AREA:PROBDEG (Day and King 2025). For waste panel saturation in the RPPCR S2-BF scenario, the list of impactful parameters is longer; also, no single parameter dominates. The list includes: S_HALITE:POROSITY; the DRZ permeability parameter DRZ_1:PRMX_LOG; the waste residual brine saturation WAS_AREA:SAT_RBRN; and factors controlling gas generation and brine consumption such as the iron corrosion rate parameter STEEL:CORRMCO2. The Castile brine pressure (CASTILER:PRESSURE) appears as a dominant parameter for only brine saturation in Replicate 3, but is considered here as it has been found to show a higher level of correspondence with brine volumes (Docherty and King 2023).

Scatter plots illustrating the sensitivity of DBR volumes to four of these parameters are shown in Figure 21 through Figure 23. Increased intact halite porosity, which is associated with both increased waste panel pressure and saturation in the RPPCR S2-BF scenario (Day and King 2025), shows some tendency to cause an increase in DBR volumes (Figure 21). Borehole permeability, which is inversely related to waste panel pressure (Day and King 2025), shows some correlation to DBR volume (Figure 22). The correlation between higher values of permeability in the DRZ and DBR volumes is likewise weak (Figure 23). Lastly, at intrusion times near the time of the previous intrusion, higher pressure in the intersected Castile brine pocket drives higher repository pressure as brine from the Castile floods the repository, strongly affecting DBR volumes. The relationship between the Castile brine pressure and S2-DBR brine releases at time 550 years (200 years post-initial intrusion) is relatively strong and is shown in Figure 24.

Information Only

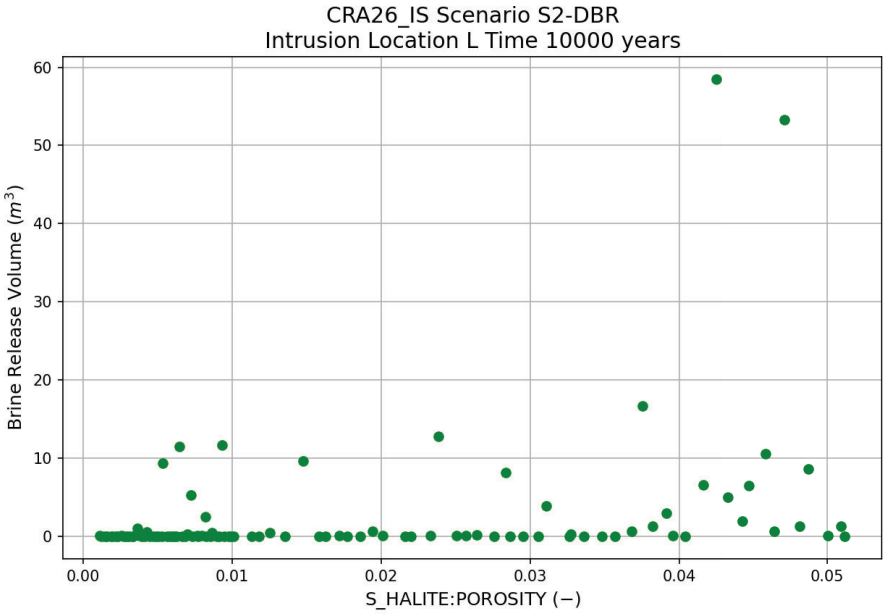

Figure 21. Halite Porosity Versus Brine Release Volume for Location "L", Scenario S2-DBR, Time 10,000 Years, Replicate 1

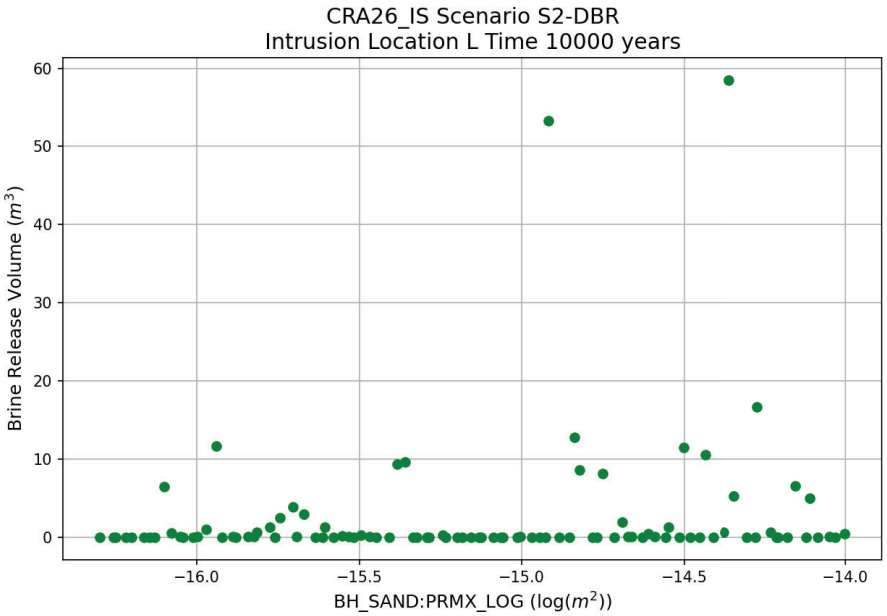

Figure 22. Borehole Permeability Versus Brine Release Volume for Location "L", Scenario S2-DBR, Time 10,000 Years, Replicate 1

Information Only

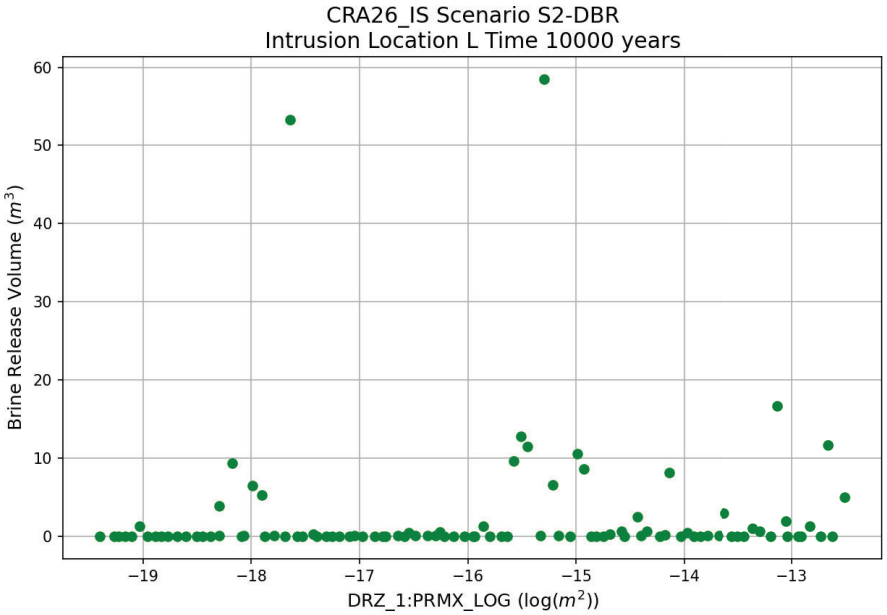

Figure 23. DRZ Permeability Versus Brine Release Volume for Location "L", Scenario S2-DBR, Time 10,000 Years, Replicate 1

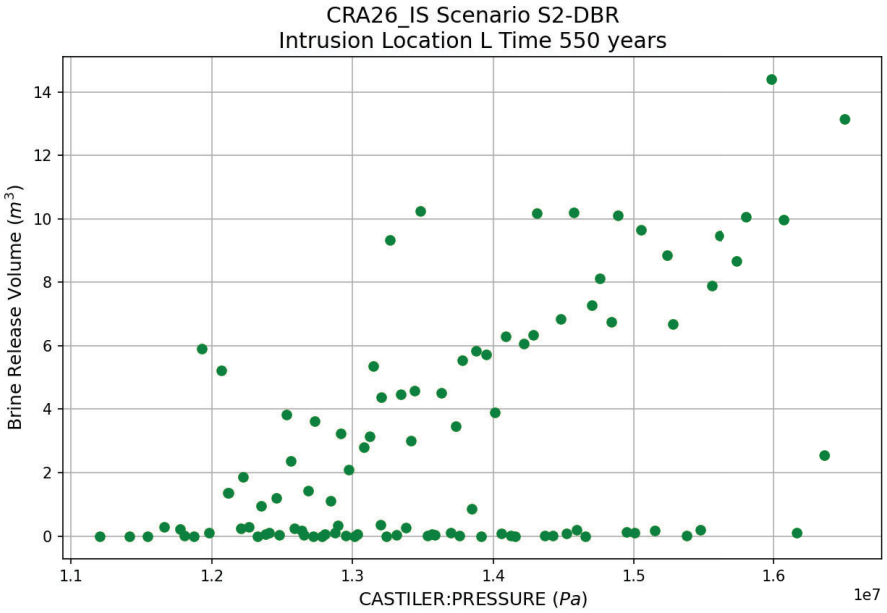

Figure 24. Castile Brine Pressure Versus Brine Release Volume for Location "L", Scenario S2-DBR, Time 550 Years, Replicate 1

Information Only

10.0 APPENDIX B – ADDITIONAL REPLICATE 1 TABLES AND PLOTS

Additional tables and plots for Replicate 1 are provided without discussion in this appendix.

10.1 S3-DBR

Table 11. S3-DBR Volume Summary, Replicate 1

Intrusion Location and Time (yr)	Mean Brine Released (m^3)		Fraction of Simulations with Non-Zero Releases		Mean of Non-Zero Brine Releases (m^3)	
	RPPCR	CRA26_IS	RPPCR	CRA26_IS	RPPCR	CRA26_IS
L	**3.73**	**1.94**	**68.00%**	**51.00%**	**5.48**	**3.81**
1200	3.32	2.02	88.00%	76.00%	3.77	2.66
1400	4.28	2.81	84.00%	69.00%	5.10	4.08
3000	4.63	2.19	62.00%	44.00%	7.46	4.98
5000	3.48	1.48	54.00%	33.00%	6.45	4.49
10000	2.94	1.21	52.00%	33.00%	5.65	3.66
M	**0.95**	**0.52**	**40.00%**	**27.20%**	**2.37**	**1.91**
1200	1.98	1.00	74.00%	59.00%	2.67	1.69
1400	1.32	0.89	61.00%	38.00%	2.16	2.33
3000	0.74	0.33	29.00%	21.00%	2.54	1.55
5000	0.30	0.25	19.00%	10.00%	1.59	2.47
10000	0.42	0.14	17.00%	8.00%	2.46	1.74
U	**0.67**	**0.25**	**15.80%**	**6.80%**	**4.22**	**3.68**
1200	1.22	0.75	19.00%	12.00%	6.45	6.26
1400	1.12	0.50	19.00%	11.00%	5.88	4.50
3000	0.56	0.00	15.00%	7.00%	3.71	0.06
5000	0.19	0.00	15.00%	2.00%	1.24	0.03
10000	0.25	0.00	11.00%	2.00%	2.23	0.01
O	**0.26**	**0.06**	**9.40%**	**3.40%**	**2.80**	**1.70**
1200	0.55	0.17	12.00%	6.00%	4.56	2.79
1400	0.46	0.11	10.00%	6.00%	4.58	1.89
3000	0.24	0.01	9.00%	3.00%	2.61	0.31
5000	0.05	0.00	8.00%	1.00%	0.57	0.00
10000	0.03	0.00	8.00%	1.00%	0.38	0.00
S3-DBR	**1.40**	**0.69**	**33.30%**	**22.10%**	**4.21**	**3.13**

Information Only

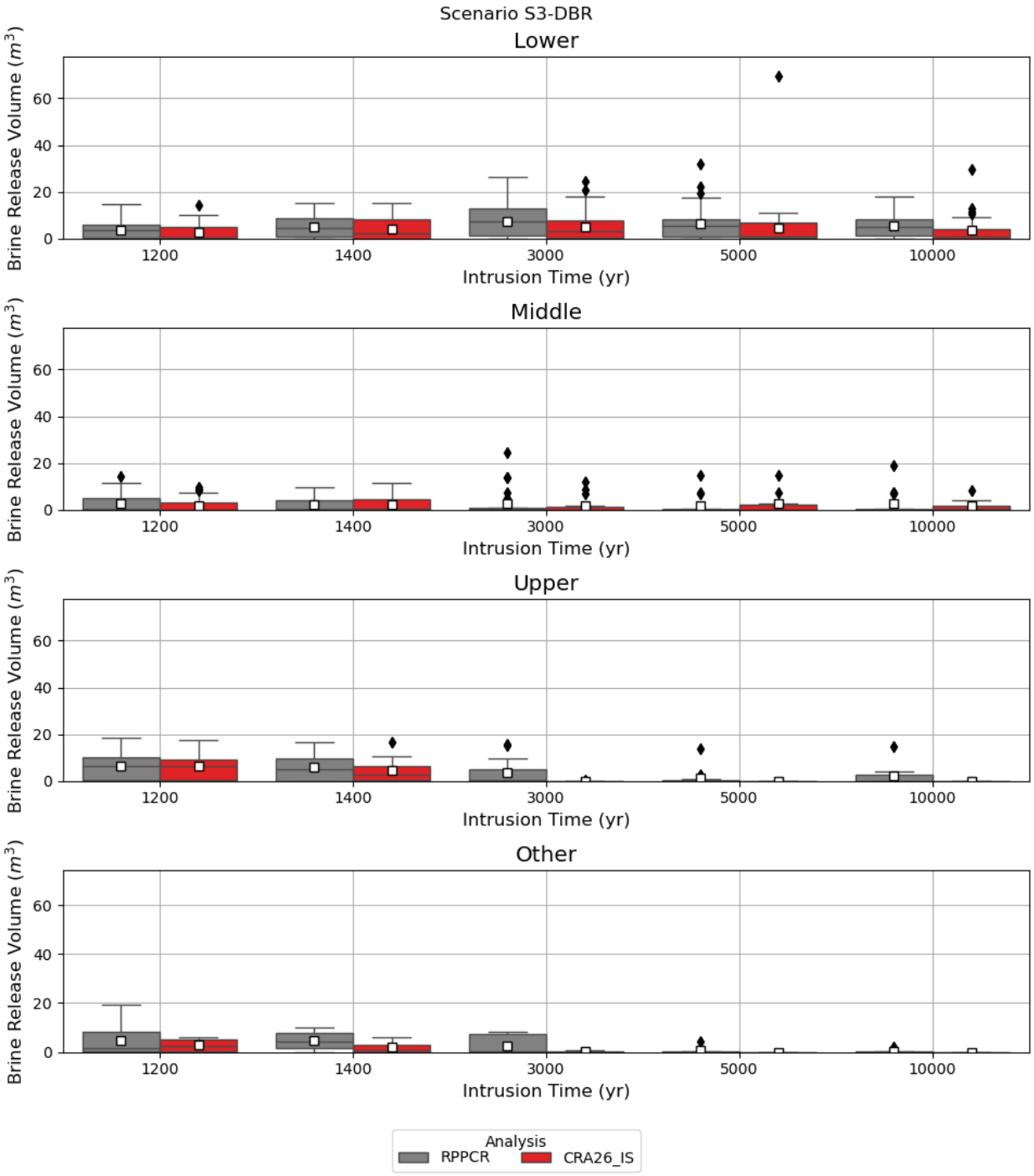

Figure 25. S3-DBR Volumes, All Non-Zero Releases, Replicate 1

Information Only

10.2 S5-DBR

Table 12. S5-DBR Volume Summary, Replicate 1

Intrusion Location and Time (yr)	Mean Brine Released (m^3)		Fraction of Simulations with Non-Zero Releases		Mean of Non-Zero Brine Releases (m^3)	
	RPPCR	CRA26_IS	RPPCR	CRA26_IS	RPPCR	CRA26_IS
L	**2.68**	**2.07**	**21.40%**	**15.20%**	**12.52**	**13.61**
1200	2.85	2.59	21.00%	17.00%	13.57	15.22
1400	2.85	2.63	21.00%	15.00%	13.58	17.53
3000	3.10	2.11	21.00%	13.00%	14.76	16.19
5000	2.85	1.15	22.00%	14.00%	12.93	8.21
10000	1.75	1.87	22.00%	17.00%	7.93	10.99
M	**1.00**	**0.40**	**14.20%**	**6.60%**	**7.04**	**6.08**
1200	1.50	1.02	18.00%	11.00%	8.36	9.30
1400	1.37	0.65	16.00%	10.00%	8.55	6.51
3000	0.90	0.13	13.00%	6.00%	6.93	2.20
5000	0.76	0.13	13.00%	3.00%	5.82	4.45
10000	0.47	0.07	11.00%	3.00%	4.27	2.24
U	**0.76**	**0.28**	**14.60%**	**6.40%**	**5.18**	**4.32**
1200	1.43	0.93	19.00%	12.00%	7.55	7.75
1400	1.32	0.44	19.00%	11.00%	6.95	3.97
3000	0.62	0.01	13.00%	5.00%	4.78	0.24
5000	0.14	0.00	12.00%	2.00%	1.16	0.07
10000	0.27	0.00	10.00%	2.00%	2.66	0.04
O	**0.28**	**0.06**	**9.40%**	**3.40%**	**2.96**	**1.79**
1200	0.59	0.18	12.00%	6.00%	4.93	2.93
1400	0.48	0.12	10.00%	6.00%	4.81	1.99
3000	0.25	0.01	9.00%	3.00%	2.78	0.32
5000	0.05	0.00	8.00%	1.00%	0.58	0.00
10000	0.02	0.00	8.00%	1.00%	0.25	0.00
S4-DBR	**1.18**	**0.70**	**14.90%**	**7.90%**	**7.91**	**8.88**

Information Only

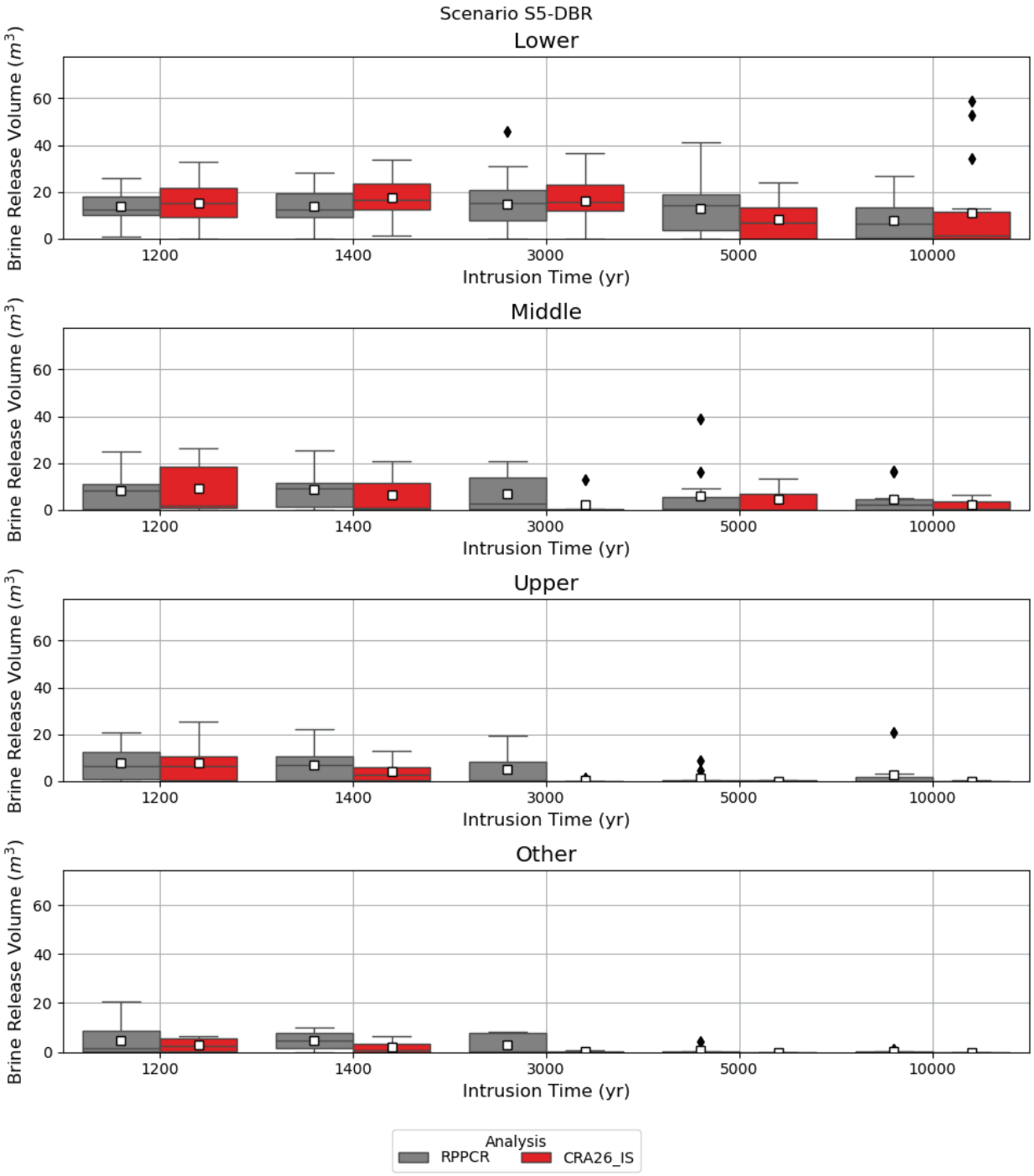

Figure 26. S5-DBR Volumes, All Non-Zero Releases, Replicate 1

Information Only

11.0 APPENDIX C –REPLICATE COMPARISON

In this appendix, select Replicate 2 and 3 results are presented and in some cases compared to the results of Replicate 1 from the CRA26_IS.

Table 13. DBR Volume Summary, Replicate 2

Intrusion Location	Mean Brine Released (m^3)		Fraction of Simulations with Non-Zero Releases		Mean of Non-Zero Brine Releases (m^3)	
	RPPCR	CRA26_IS	RPPCR	CRA26_IS	RPPCR	CRA26_IS
S1-DBR	**0.61**	**0.32**	**10.25%**	**4.46%**	**5.98**	**7.17**
L	1.58	0.84	16.83%	8.83%	9.39	9.52
M	0.41	0.19	7.83%	3.50%	5.29	5.35
U	0.36	0.21	9.00%	3.83%	4.01	5.46
O	0.09	0.04	7.33%	1.67%	1.28	2.48
S2-DBR	**2.21**	**1.37**	**37.55%**	**27.35%**	**5.89**	**5.01**
L	5.27	3.67	72.80%	60.40%	7.24	6.07
M	2.88	1.44	54.00%	40.40%	5.34	3.56
U	0.60	0.35	15.20%	7.00%	3.97	4.96
O	0.09	0.03	8.20%	1.60%	1.15	1.70
S3-DBR	**1.50**	**0.87**	**32.50%**	**20.95%**	**4.61**	**4.16**
L	3.73	2.44	64.60%	49.40%	5.77	4.94
M	1.41	0.73	38.80%	25.60%	3.62	2.85
U	0.70	0.27	15.40%	6.40%	4.55	4.23
O	0.17	0.05	11.20%	2.40%	1.47	1.88
S4-DBR	**0.81**	**0.51**	**14.05%**	**7.45%**	**5.75**	**6.78**
L	1.99	1.28	21.80%	14.60%	9.13	8.74
M	0.72	0.46	13.00%	7.00%	5.57	6.63
U	0.43	0.26	13.20%	6.40%	3.26	4.00
O	0.09	0.03	8.20%	1.80%	1.08	1.43
S5-DBR	**1.08**	**0.56**	**16.30%**	**7.00%**	**6.65**	**7.99**
L	2.52	1.48	25.80%	13.80%	9.76	10.71
M	0.98	0.46	13.80%	5.60%	7.08	8.14
U	0.67	0.26	14.20%	6.20%	4.69	4.18
O	0.18	0.05	11.40%	2.40%	1.55	1.89
All Scenarios						
L	**2.96**	**1.90**	**39.46%**	**28.62%**	**7.51**	**6.63**
M	**1.25**	**0.64**	**24.81%**	**15.92%**	**5.03**	**4.00**

Information Only

Intrusion Location	Mean Brine Released (m^3)		Fraction of Simulations with Non-Zero Releases		Mean of Non-Zero Brine Releases (m^3)	
	RPPCR	CRA26_IS	RPPCR	CRA26_IS	RPPCR	CRA26_IS
U	0.54	0.27	13.23%	5.88%	4.12	4.52
O	0.12	0.04	9.19%	1.96%	1.33	1.89
ALL	1.22	0.71	21.67%	13.10%	5.63	5.42

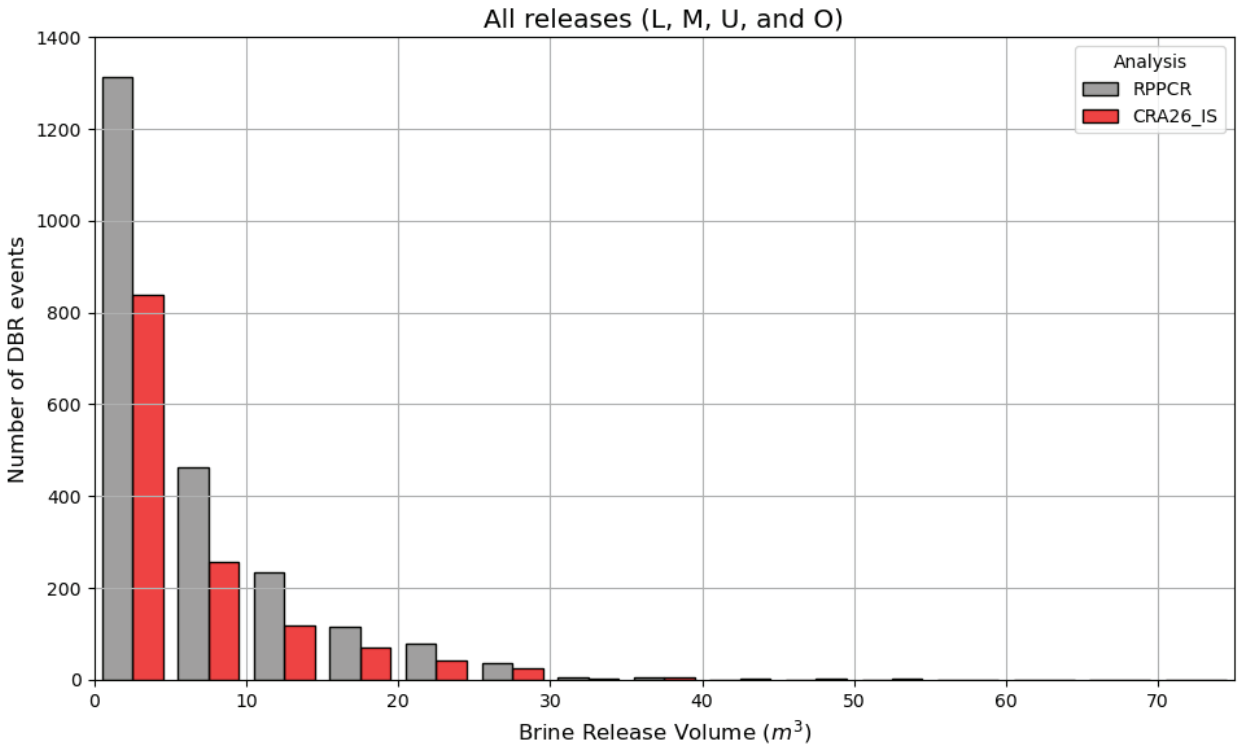

Figure 27. Release Volume Frequency, All Non-Zero Releases, Replicate 2

Information Only

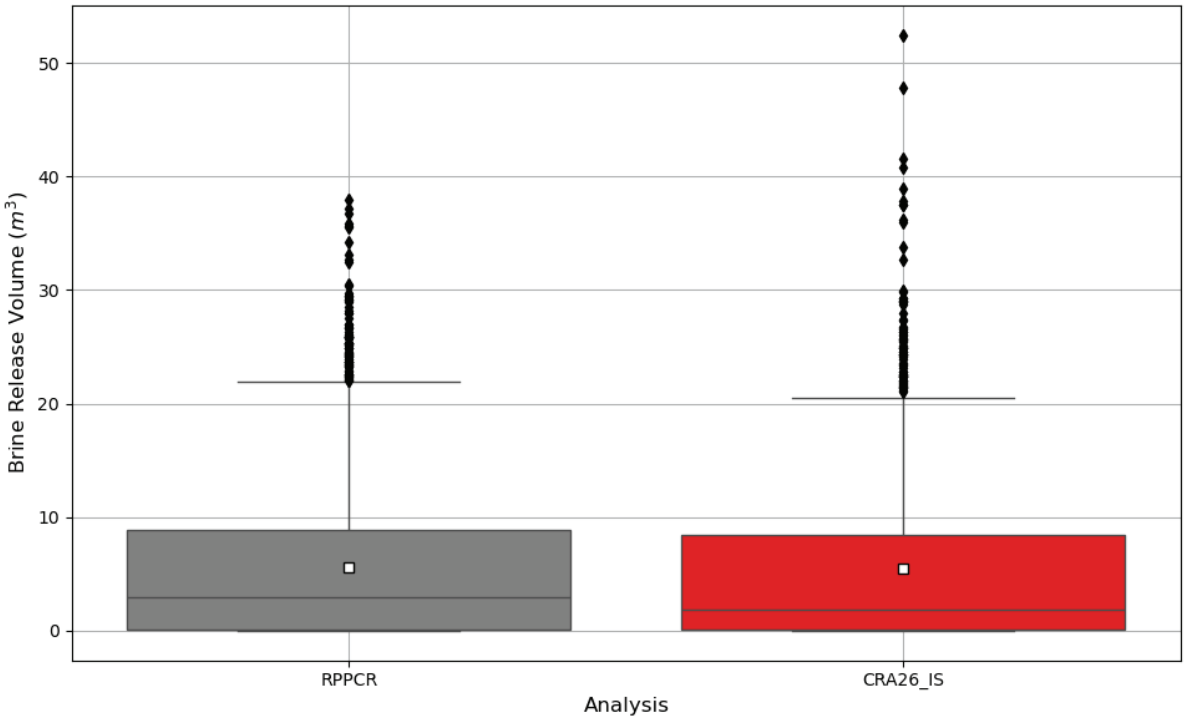

Figure 28. Release Volumes, All Non-Zero Releases, Replicate 2

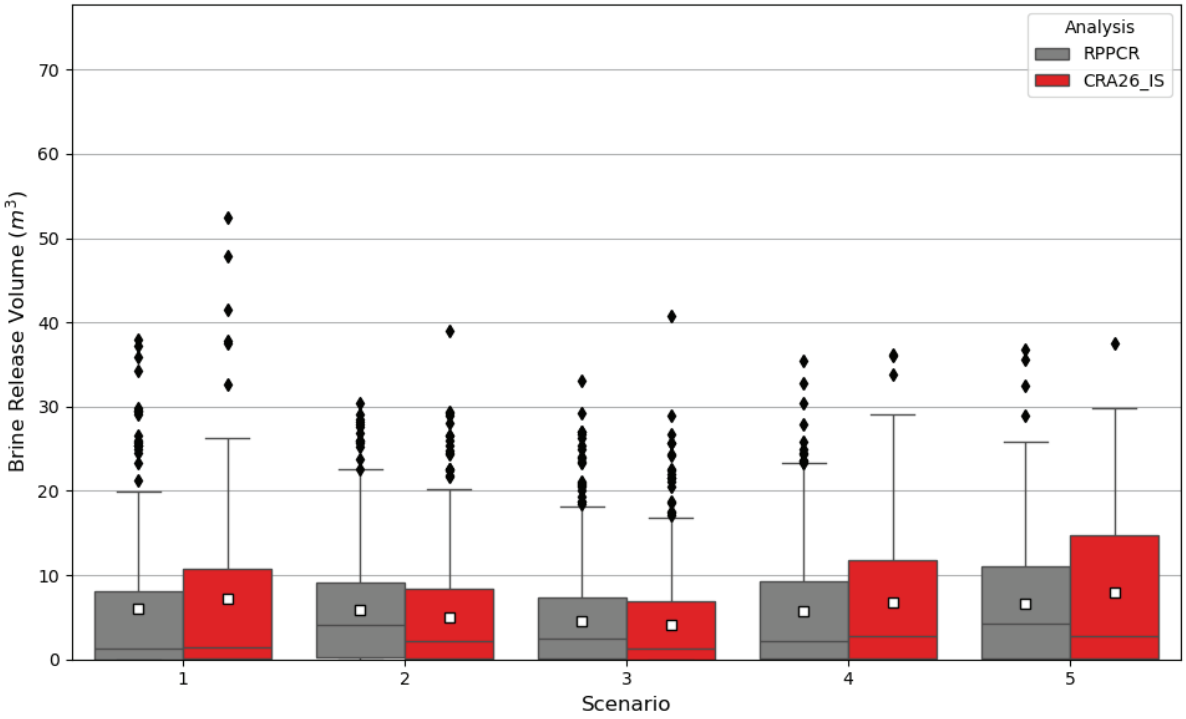

Figure 29. Release Volumes by Scenario, All Non-Zero Releases, Replicate 2

Information Only

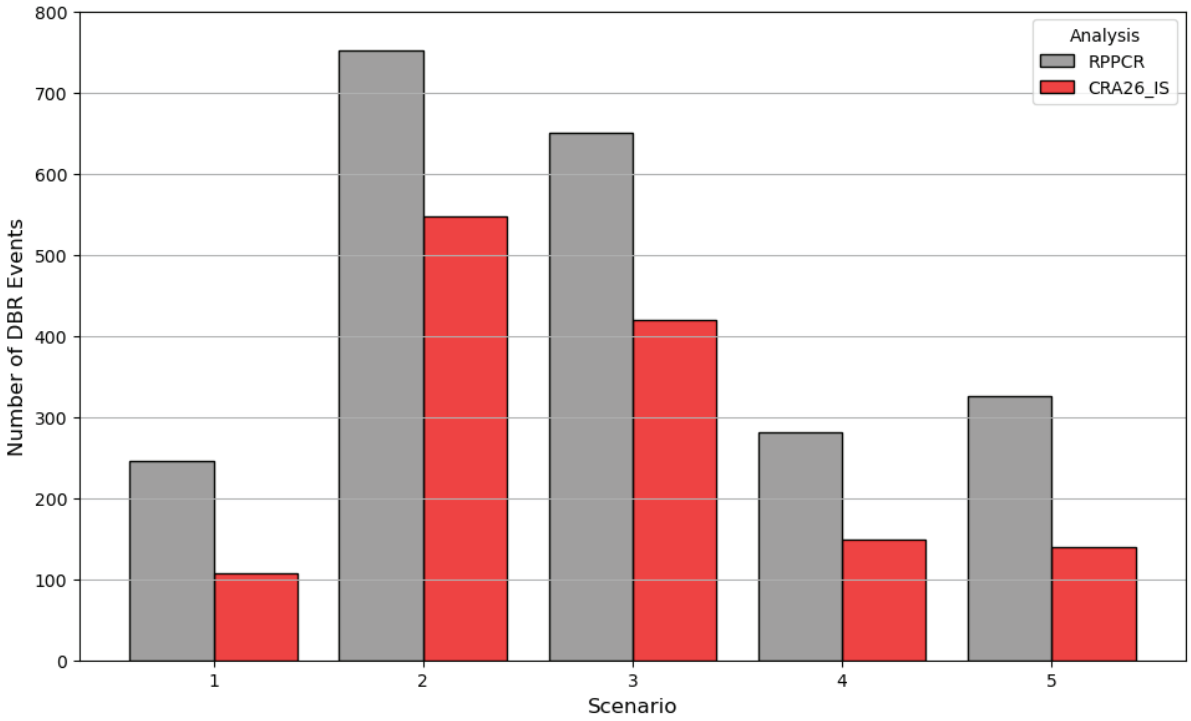

Figure 30. Number of Non-Zero DBR Events by Scenario, Replicate 2

Information Only

Table 14. DBR Volume Summary, Replicate 3

Intrusion Location	Mean Brine Released (m^3)		Fraction of Simulations with Non-Zero Releases		Mean of Non-Zero Brine Releases (m^3)	
	RPPCR	CRA26_IS	RPPCR	CRA26_IS	RPPCR	CRA26_IS
S1-DBR	**0.45**	**0.21**	**9.54%**	**4.75%**	**4.71**	**4.39**
L	1.19	0.55	15.00%	9.00%	7.93	6.13
M	0.27	0.12	7.17%	4.00%	3.79	3.12
U	0.25	0.12	9.33%	4.33%	2.73	2.68
O	0.08	0.04	6.67%	1.67%	1.24	2.49
S2-DBR	**2.10**	**1.19**	**38.45%**	**27.55%**	**5.46**	**4.33**
L	5.38	3.28	75.40%	61.20%	7.14	5.35
M	2.33	1.16	56.60%	37.60%	4.12	3.08
U	0.53	0.29	14.20%	9.00%	3.75	3.28
O	0.15	0.04	7.60%	2.40%	1.92	1.72
S3-DBR	**1.39**	**0.70**	**33.85%**	**22.15%**	**4.11**	**3.18**
L	3.74	2.10	66.40%	51.80%	5.63	4.05
M	1.17	0.48	43.00%	25.60%	2.73	1.86
U	0.47	0.18	15.00%	8.00%	3.15	2.21
O	0.18	0.06	11.00%	3.20%	1.61	1.95
S4-DBR	**0.63**	**0.30**	**11.65%**	**6.70%**	**5.41**	**4.51**
L	1.52	0.82	18.00%	12.00%	8.47	6.87
M	0.46	0.17	9.40%	6.40%	4.89	2.71
U	0.40	0.17	11.80%	6.40%	3.40	2.71
O	0.13	0.04	7.40%	2.00%	1.81	1.83
S5-DBR	**0.79**	**0.36**	**13.45%**	**6.95%**	**5.89**	**5.17**
L	2.08	1.03	19.80%	13.20%	10.51	7.79
M	0.44	0.18	10.60%	5.00%	4.17	3.62
U	0.49	0.17	13.00%	7.00%	3.77	2.40
O	0.16	0.06	10.40%	2.60%	1.51	2.25
All Scenarios						
L	**2.72**	**1.52**	**38.00%**	**28.65%**	**7.16**	**5.30**
M	**0.91**	**0.41**	**24.65%**	**15.27%**	**3.69**	**2.69**
U	**0.42**	**0.18**	**12.54%**	**6.85%**	**3.38**	**2.67**
O	**0.14**	**0.05**	**8.54%**	**2.35%**	**1.61**	**2.04**
ALL	**1.05**	**0.54**	**20.93%**	**13.28%**	**5.01**	**4.07**

Information Only

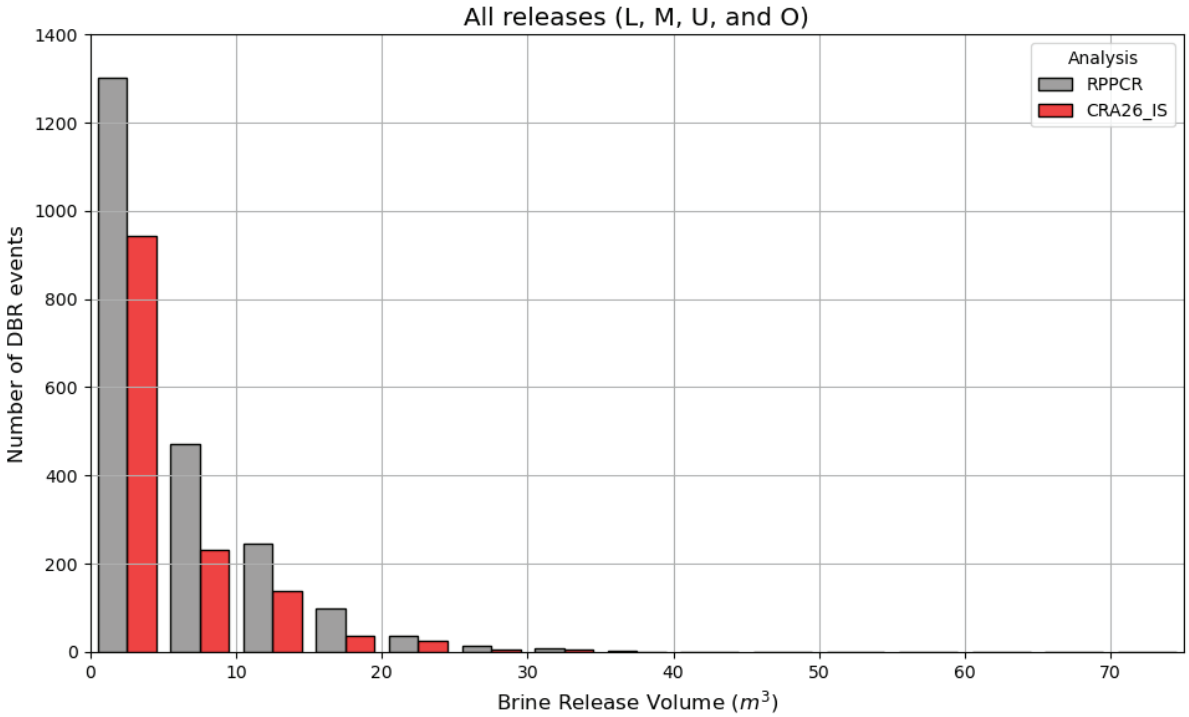

Figure 31. Release Volume Frequency, All Non-Zero Releases, Replicate 3

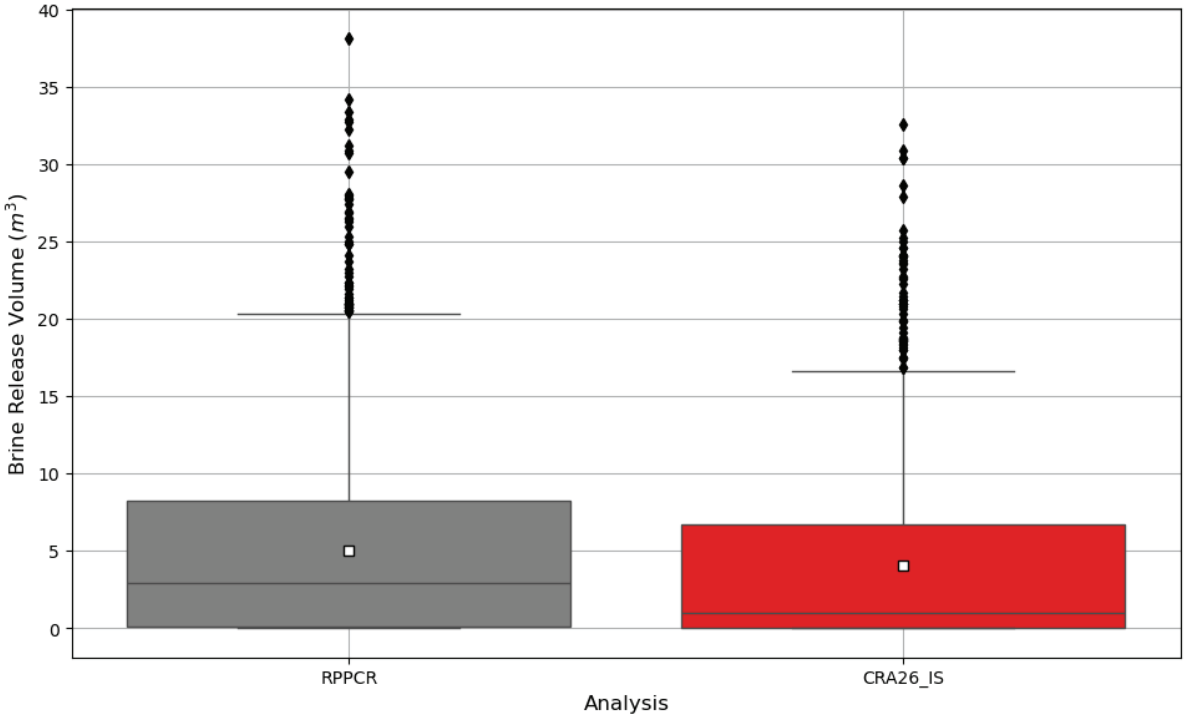

Figure 32. Release Volumes, All Non-Zero Releases, Replicate 3

Information Only

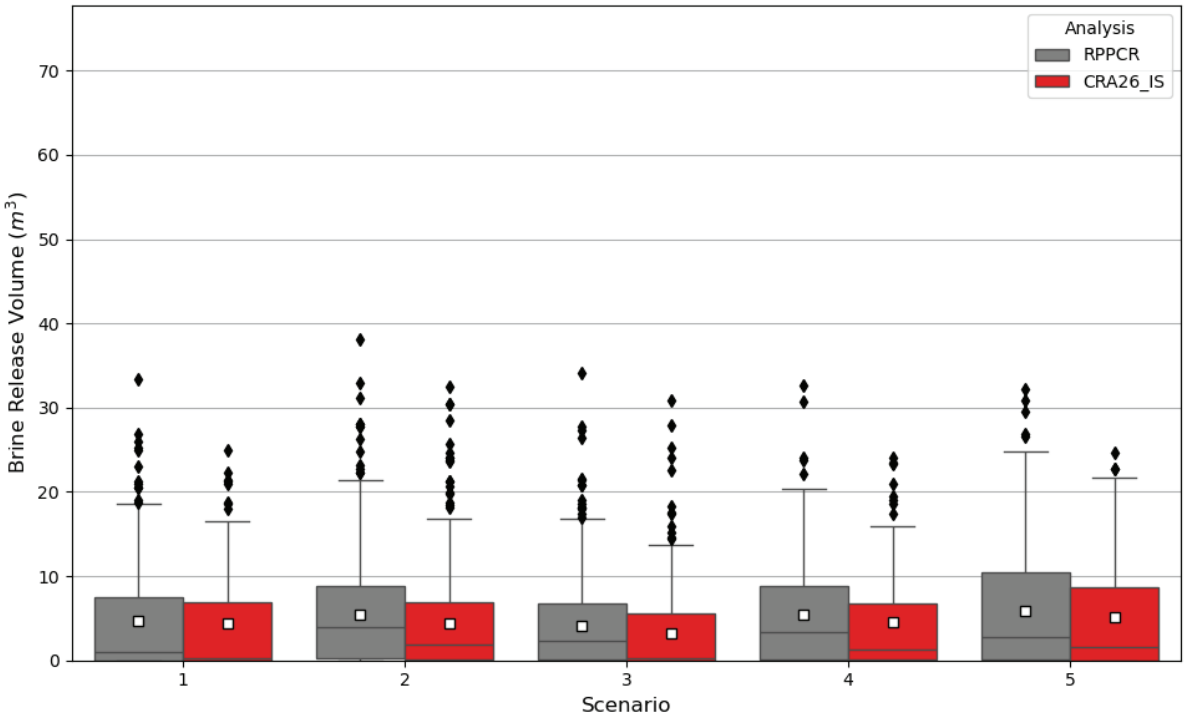

Figure 33. Release Volumes by Scenario, All Non-Zero Releases, Replicate 3

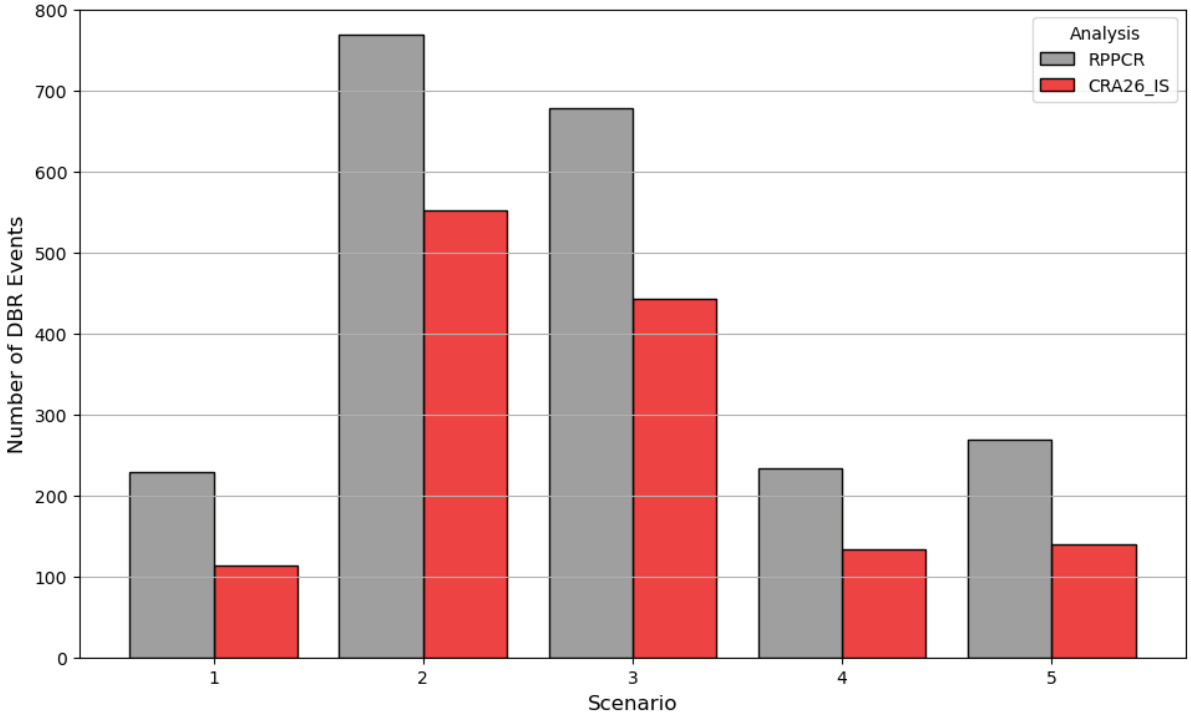

Figure 34. Number of Non-Zero DBR Events by Scenario, Replicate 3

Information Only

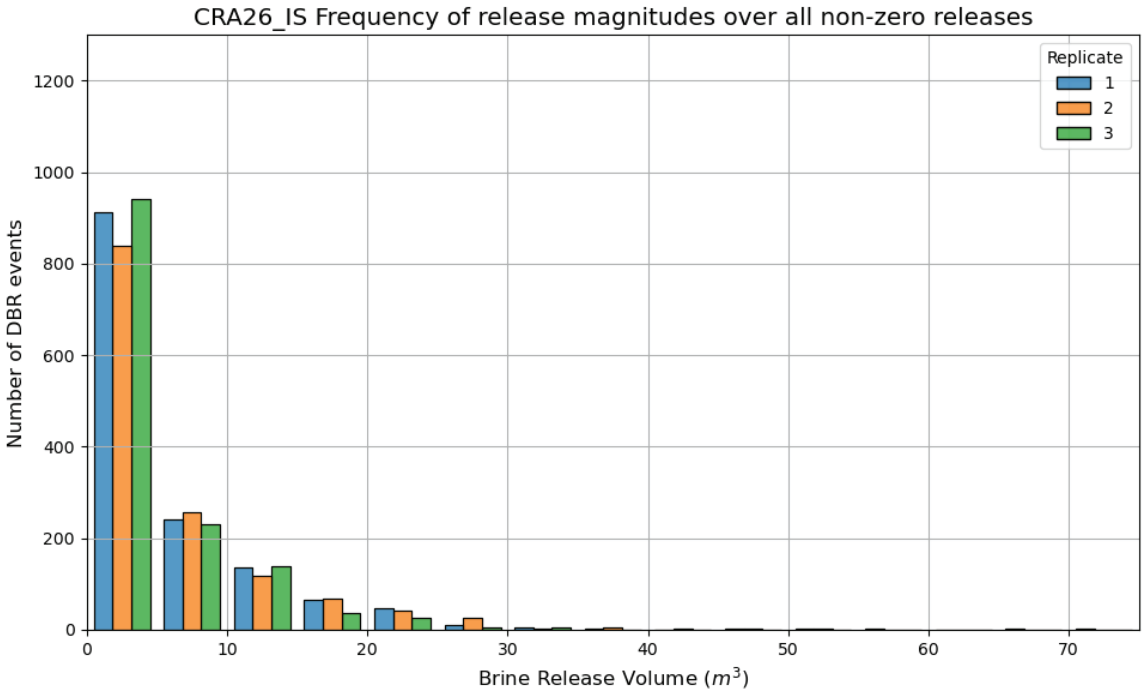

Figure 35. Release Volume Frequency, All Non-Zero Releases, All Replicates

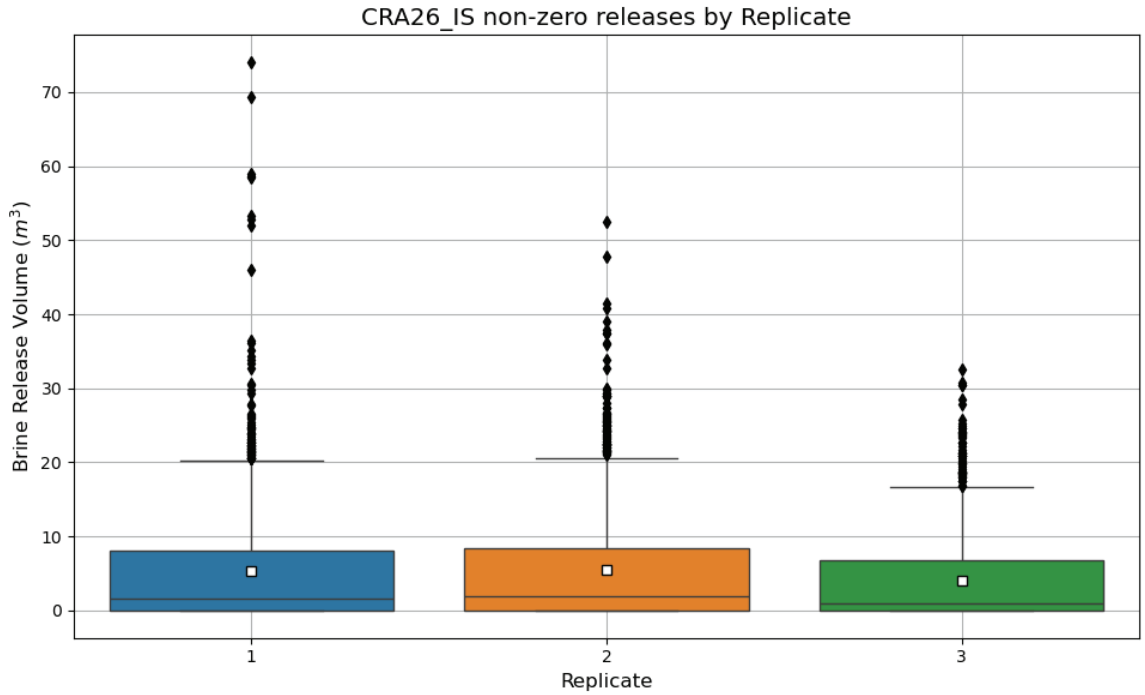

Figure 36. Release Volumes, All Non-Zero Releases, All Replicates

Information Only

Sandia National Laboratories is a multimission laboratory managed and operated by National Technology & Engineering Solutions of Sandia, LLC, a wholly owned subsidiary of Honeywell International Inc., for the U.S. Department of Energy's National Nuclear Security Administration under contract DE-NA0003525. This research is funded by WIPP programs administered by the Office of Environmental Management (EM) of the U.S. Department of Energy.







Information Only